NINETEENTH EUROPEAN ROTORCRAFT FORUM

Paper n° C17

ON THE UNSTEADY AERODYNAMICS OF HIGHER HARMONIC CONTROL

by

E. R. Wood, M. F. Platzer,
A. Abourahma, & M. A. Couch

Naval Postgraduate School
Monterey, California
U.S.A. 93943

September 14-16, 1993
CERNOBBIO (Como)
ITALY

ASSOCIAZIONE INDUSTRIE AEROSPAZIALI
ASSOCIAZIONE ITALIANA DI AERONAUTICA ED ASTRONAUTICA

ON THE UNSTEADY AERODYNAMICS OF HIGHER HARMONIC CONTROL

by

E. Roberts Wood, Max F. Platzer
Ahmed Abourahma, Mark A. Couch

Department of Aeronautics & Astronautics
Naval Postgraduate School
Monterey, California 93943
U.S.A.

ABSTRACT

Open loop performance data from the OH-6A higher harmonic control (HHC) flight test program, Wood et al.[1], show significant reductions in main rotor shaft torque and engine power in the airspeed regime from hover to 100 knots. Depending upon HHC controller phase and helicopter airspeed, reductions in power were recorded as large as 20%, with reductions of the order of 10% being typical.

The authors consider the unsteady aerodynamics of HHC, including wake effects, in order to research whether such power reductions are feasible with higher harmonic control. Both classical closed-form methods and a numerical panel code are applied. While it has long been recognized that an airfoil oscillating in plunge can achieve propulsive force ("Katzmayr effect", Garrick [2]), this paper shows that the effect can be enhanced by a factor of two or more when in the presence of layers of shed vorticity of the proper phase. In addition, while Garrick's [2] work shows that an airfoil oscillating in pitch will typically produce drag at most values of reduced frequency, k, it is found that the presence of another layer of shed vorticity of the proper phase can: (1) reduce the drag on the pitching airfoil and depending upon wake spacing, reduced frequency, and phase, may even provide propulsive force acting on the airfoil similar to the "Katzmayr" effect for plunging airfoils.

1. INTRODUCTION

Higher harmonic control (HHC) is an active vibration control concept for helicopters, which alters the aerodynamic loads on the rotor blades such that the blade response is reduced. This, in turn, reduces the vibratory forces and moments acting at the hub, which cause airframe vibration. HHC flight test results such as those given in Ref. [1] show that by this means up to a 90 percent reduction in helicopter airframe vibration levels can be achieved. Basically, HHC is an electronic, computer-controlled active vibration suppression system which senses and cancels vibrations in a helicopter by N/revolution feathering or pitch motion of the rotor blades, N being the number of blades.

Figures 1 and 2 (from Ref.[1]) show the very substantial vibration reduction achieved under a NASA-Army sponsored program using a modified OH-6A helicopter. Higher harmonic blade pitch control was achieved by superimposing 4/rev. (32 Hz) swashplate motion upon basic cyclic and collective control inputs. The aircraft was flown from zero airspeed to 100 knots with the HHC system operated both open loop (manually) and closed loop (computer controlled).

In the program described in Ref.[1], in addition to reducing vibration levels, the HHC system also showed the potential for decreased helicopter power requirements. Figure 3 shows the status of the effect of HHC on performance at the low end of the airspeed regime, or in hover. Figs. 3(a) and 3(b) show hover power required for three different schedules of HHC open loop excitation. As would be expected in a hover, the polar plots reduce to circles. ***What is of interest is that the amount of power reduction achieved, of the order of 10% or 20 horsepower, appears to be relatively independent of the type of excitation applied.***

Figures 4(a) and 4(b) from Wood et al. [3] show the effect of HHC on measured helicopter performance at 60 knots indicated airspeed. Results are presented for lateral swashplate excitation equivalent to $\pm$ 0.33 degrees of blade angle. Given is a polar plot showing power required as measured by either main rotor shaft torque or engine torque pressure. Figure 4(a) shows the effect of HHC on main rotor shaft torque while Figure 4(b) shows the corresponding effect on engine power. The data was recorded as the 4P command phase to the HHC actuators was varied in 30-

degree increments. After establishing the baseline power levels, which were those for "HHC off", the zero phase condition was the first data point recorded with "HHC on". The next was that at 30 degree phase, etc., concluding with recording the performance parameters at the 360-degree controller phase setting.

The 60-knot data presented shows certain characteristics that were typical of all the open loop data taken in forward flight during the program. We first note that the two plots, Figs. 4(a) and 4(b) are identical. This finding would rule out any skepticism as to the reliability of the transducers used for the two separate readings. Also, this tells us that the reduction in main rotor shaft torque is not being achieved at the expense of engine power, since Fig. 4(b) indicates that there is a net savings in engine power over and above that required to drive the HHC system. In fact, the power savings is significant at about 10% to 15% of total power.

1. Main rotor shaft torque and engine power at a given airspeed vary significantly with the phase setting of the open-loop manual controller.

2. At certain phase settings there appears to be a significant reduction in main rotor shaft torque and engine power.

3. The shaft torque and engine power readings recorded with "HHC on" at zero-degree phase angle were made at the beginning and end of the approximately 20-minute test sequence and we find the closure is poor.

Fig. 5(a) and Fig. 5(b) show the power reduction achieved by HHC at 80 knots level flight. For Figure 5, main rotor shaft torque and engine torque pressure are presented similar to Figure 4. Again, we note the good agreement between the shaft torque plot and the engine torque pressure plot. Similar to 60 knots, we observe a significant reduction in power required with "HHC on".

Fig. 6(a) and Fig. 6(b) show the effect of HHC on main rotor shaft torque and engine torque pressure for 100 knots indicated airspeed. Figure 6 in contrast to Figures 4 and 5, ***indicates negligible reduction in power at 100 knots airspeed.***

From Figures 3, 4, 5 and 6 we are left to conclude that a substantial reduction in power can be achieved by application of HHC in hover and forward flight. The amount of power saved seems to be of the order of 10% in hover increasing to about 15% in the region from 60 to 80 knots and diminishing to small values at higher airspeeds, as we move out past 100 knots.

2. UNSTEADY AERODYNAMICS AND HHC

Recent studies of the OH-6A flight test data indicate that the mechanism by which the power reduction was achieved is related to the unsteady aerodynamics associated with HHC. This is supported by the fact that higher harmonic control by the very nature of the method by which it is implemented through oscillating an airfoil in pitch with resulting plunge motion, requires definition of unsteady aerodynamics to adequately model its physics.

Second, our present knowledge base of rotary wing unsteady aerodynamics still remains limited. The fundamental closed form solutions by Theodorsen [4] and Loewy [5] provide the basis for theoretical work in this area. While Loewy's work on wake-induced flutter helps explain the phenomenon, it also points up the difficulties to be overcome. That is, ***the closed form theory shows rapid changes in the lift deficiency function with changes in reduced frequency, k; wake spacing, h; and frequency ratio, m.***

Third, there have been tremendous advances made in computation since the time of Loewy's work (1957). Yet, there has been little motivation in the past thirty years to extend this work, because it has been within the state-of-the-art to design a rotor blade that is free of flutter. However, increased interest in higher harmonic control and its potential benefits for the helicopter now encourage us to try to advance the boundaries of the knowledge of rotary wing unsteady aerodynamics.

In the past, emphasis in the study of unsteady aerodynamics has tended to focus on flutter instability and the effect of unsteady aerodynamics on generating lift and torsional loads. Here, because we are interested in performance, ***emphasis will be on the effect of unsteady aerodynamics on the drag of the airfoil.*** When the drag force is reversed, acting to propel the airfoil forward, it is generally referred to as either negative drag or propulsive force. The classic report on this subject is that by Garrick [2].

The specific mechanisms to be discussed are:

1. The unsteady aerodynamics associated with a plunging airfoil and how that produces a propulsive force or decrease in rotor power.

2. The influence of a layer of wake vorticity on this propulsive force, which represents the influence of the unsteady aerodynamics of one rotor blade on adjacent rotor blades.

3. The unsteady aerodynamics associated with an airfoil oscillating in pure pitch and how this produces in general a drag force on the airfoil unless accompanied by layers of shed wake vorticity.

4. The influence of the phasing of a layer of shed vorticity on this drag force, and how, depending upon phase its effect on the airfoil will either result in a drag force or a propulsive force.

The analysis of the above effects will be based upon two approaches:

(1) The classical flat plate unsteady aerodynamic theory for incompressible fluids of Theodorsen [4] and its extension to include the rotor wake of Loewy [5].

(2) A newly developed panel method by Platzer et al. [6], that can be applied for unsteady incompressible flow past airfoils or airfoil combinations of arbitrary geometry.

In one approach, Theodorsen's well known lift deficiency function C(k) has been modified by Loewy for the case of the hovering rotor. Airfoil drag or propulsive force is determined by the methods of Garrick [2]. In the other approach, a panel computer code has been developed which allows the systematic study of the lift and drag characteristics produced by oscillating airfoils and airfoil combinations in incompressible inviscid flow.

3. BACKGROUND

Unsteady Aerodynamics and Airfoil Drag

The effect of pitch and plunge oscillations on the resultant drag of an airfoil has been the object of aeroelastic research dating back to World War I. One of the earliest investigators of this phenomenon was R. Katzmayr [7], who in 1922 conducted two series of experiments to explore the effects of oscillatory fluid or airfoil motion on resultant lift and drag. In his second series of experiments, the airfoils were stationary while the airflow itself was subjected to periodic oscillations. Here, for certain velocities and frequencies, and considering thick airfoil sections, Katzmayr measured negative drag or positive propulsive force. This discovery, to be later known as "Katzmayr effect", helped to answer questions on the propulsive mechanisms of birds flying through the air. Later, E. G. Richardson [8] used the "Katzmayr effect" to explain the locomotion of fish through water.

The most relevant work to date with respect to this paper was that by I. E. Garrick [2]. Garrick applied the work of Theodorsen [4] to a method developed by von Karman and Burgers [9] to obtain a closed form analytical expression for the propulsive force generated by an oscillating airfoil. An airfoil in pure plunge or flapping motion was shown by Garrick to have a propulsive force throughout the entire range of reduced frequency, k, defined by

$$k = \frac{b\omega}{V}$$

The expression for propulsive force was shown to be

$$P_x = \pi \rho b \omega^2 h_o^2 (F^2 + G^2)$$

where ρ is the density of air, b is semi-chord, and F(k) and G(k) constitute Theodorsen's lift deficiency function, C(k), given by

$$C(k) = F(k) + iG(k)$$

For the special case of pure pitch the horizontal force is given by

$$P_x = \pi \rho b^3 \omega^2 \alpha_o^2 \left\{ \left(F^2 + G^2\right)\left[\frac{1}{k^2} + \left(\frac{1}{2} - a\right)^2\right] + \frac{1}{2}\left(\frac{1}{2} - a\right) - \frac{F}{k^2} - \left(\frac{1}{2} - a\right)\frac{G}{k} \right\}$$

These results are summarized by Garrick in Figure 7 which plots the ratio of average increase in kinetic energy in the wake to work done per unit time versus 1/k. If **E/W** is less than one, then propulsive force results from the motion. This shows that an airfoil oscillating in plunge produces a propulsive force ("Katzmayr effect"), whereas for an airfoil oscillating in pitch, propulsive force can only be achieved for a specified range of reduced frequency values and centers of rotation (***a***), where k must be greater than about 0.67.

Unsteady Aerodynamics and the Helicopter

Given in Figure 8 is a semi-logarithmic plot of Theodorsen's lift deficiency function versus reduced frequency, k. If we concern ourselves with the "n" per revolution excitation associated with higher harmonic control, we find the region of interest to be confined to only one part of the plot for modern day helicopters. This is given by the range of reduced frequency values from k = .08 to k = 0.5. These points are shown for the helicopters identified on the plot. A typical helicopter reduced frequency value would be k = 0.1. For the OH-6A flown for the NASA/Army HHC tests, the value for k is 0.1234 (r/R = 0.7).

Figure 8 is restricted to the case where there is very large spacing between rotor wakes. It is well recognized that for realistic wake spacings, one should refer to Loewy's modified lift deficiency function, C′(k), which accounts both for wake spacing and for phasing of the wake vorticity with respect to the reference blade. This is indicated in Figure 9 which shows Loewy's lift deficiency function over a range of k values, and plotted for a number of wake spacing positions, including the limiting case where h = 0 and all layers of wake vorticity lie in the plane of the rotor. Also shown is the case where h equals infinity which corresponds to Theodorsen's theory, as can be seen by comparison of that line on the plot with Figure 8. Loewy in Ref. [5] has shown that for finite wake spacings, the frequency ratio parameter, m, is important, and it should be emphasized that Figure 9 represents the case for only one frequency ratio, where m equals zero.

4. ANALYSIS

Theodorsen's Lift Deficiency Function

The aerodynamic forces and moments on an oscillating airfoil for the fixed-wing case as determined by Theodorsen [4] are based on potential flow theory and the Kutta condition. In the manner suggested by Scanlan and Rosenbaum [10], the total pressure difference is obtained by adding the pressure differences for the non-circulatory and circulatory terms.

$$\frac{\Delta p(x)}{\rho V} = \frac{2}{\pi}\left[1 - C(k)\right]\int_{-1}^{1}\sqrt{\frac{1-x}{1+x}}\sqrt{\frac{1+\xi}{1-\xi}}\, w(\xi)\, d\xi + \frac{2}{\pi}\int_{-1}^{1}\sqrt{\frac{1-x}{1+x}}\sqrt{\frac{1+\xi}{1-\xi}}\left(\frac{1}{x-\xi}\right)d\xi$$
$$- \frac{ik}{2}\log\left[\frac{1 - x\xi - \sqrt{1-x^2}\sqrt{1-\xi^2}}{1 - x\xi + \sqrt{1-x^2}\sqrt{1-\xi^2}}\right] w(\xi)\, d\xi$$

where a lift deficiency function is defined as

$$C(k) = \frac{\displaystyle\int_1^{\infty} \frac{x_o}{\sqrt{x_o^2 - 1}}\, e^{-ikx_o}\, dx_o}{\displaystyle\int_1^{\infty} \frac{x_o + 1}{\sqrt{x_o^2 - 1}}\, e^{-ikx_o}\, dx_o}$$

The analytical solution to the lift deficiency function involves the use of complex Bessel functions (or Hankel functions), and can be written as

$$C(k) = \frac{H_1^{(2)}}{H_1^{(2)} + i H_0^{(2)}}$$

where $\mathbf{H_n^{(2)}=J_n-iY_n}$, which is the Hankel function of the second kind of order n. The lift deficiency function can be separated into its real and imaginary parts as $\mathbf{C(k) = F(k) + iG(k)}$, where

$$F(k) = \frac{J_1 (J_1 + Y_0) + Y_1 (Y_1 - J_0)}{(J_1 + Y_0)^2 + (Y_1 - J_0)^2}$$

$$G(k) = - \frac{Y_1 Y_0 + J_1 J_0}{(J_1 + Y_0)^2 + (Y_1 - J_0)^2}$$

and all Bessel functions are evaluated at reduced frequency, k. If a semi-logarithmic plot of Theodorsen's functions F(k) and G(k) is used as shown in Figure 8, the limits of F(k) and G(k) as $k \to 0$ and $k \to \infty$ can be more easily seen. Mathematically, it is interesting to note that when $\partial \mathbf{G}/\partial \mathbf{k} = \mathbf{0}$, k = -G = 0.188773655....

Loewy's Lift Deficiency Function

The aerodynamic forces and moments on an oscillating airfoil for the rotary-wing case are more complex than the fixed-wing counterpart. Loewy [5] determines these forces and moments, but uses a slightly different approach to the problem by solving the integral downwash equation which leads to an equation for the pressure distribution which is in the same form as Theodorsen.

To account for the wakes generated by the previous blades in the same revolution and all blades in previous revolutions. He uses two indices to account for the vorticity shed by a given wake: n indicates the revolution and q indicates the blade whose wake it is. The induced velocity or downwash resulting from an element of vorticity is obtained from the Biot-Savart Theorem. Loewy shows that the vorticity shed by the qth blade in the nth revolution is

$$\gamma_{nq} = i k \Gamma e^{\left[i (\psi_q - k\xi - 2\pi m q/Q - 2\pi m n)\right]}$$

where Γ is the total circulation around the airfoil, ψ_q is the phase angle by which the motion of the qth blade leads that of the reference blade, and m is the ratio of oscillatory frequency to rotational frequency.

Writing the integrals involving the bound vorticity and the vorticity in the wake of the reference airfoil separately from the rows of vorticity below the plane of the rotor yields

$$\begin{aligned} w(x) = -\frac{1}{2\pi}\Bigg[& \int_{-1}^{1} \frac{\gamma_a(\xi)\, d\xi}{x-\xi} - i k \Gamma \int_{1}^{\infty} \frac{e^{-ik\xi}\, d\xi}{x-\xi} \\ & - i k \Gamma \sum_{q=1}^{Q-1} e^{-i(2\pi m q/Q - \psi_q)} \sum_{n=0}^{\infty} e^{-i 2\pi m n} \int_{-\infty}^{\infty} \frac{e^{-ik\xi}\,(x-\xi)\, d\xi}{(x-\xi)^2 + (nQ+q)^2 h^2} \\ & - i k \Gamma \sum_{n=1}^{\infty} e^{-i 2\pi m n} \int_{-\infty}^{\infty} \frac{e^{-ik\xi}\,(x-\xi)\, d\xi}{(x-\xi)^2 + n^2 Q^2 h^2} \Bigg] \end{aligned}$$

In essence the problem has been broken down in the same manner as Theodorsen. The first integral represents the effects of the freestream on the airfoil (non-circulatory terms). The second integral represents the velocity created by the vorticity generated by the reference wake (circulatory term). The third and fourth integrals represent the velocity created by the vorticity generated by previous blades or in previous revolutions (circulatory terms). The last two integrals have the form

$$\int_{-\infty}^{\infty} \frac{e^{-ik\xi}\,(x-\xi)\,d\xi}{(x-\xi)^2 + A^2} = i\pi e^{-k(ix+A)}$$

Substituting this expression into the downwash equation and noting that the summations over *n* are convergent geometric series give

$$w(x) = -\frac{1}{2\pi}\left[\int_{-1}^{1} \frac{\gamma_a(\xi)\,d\xi}{(x-\xi)} - ik\Gamma\int_{1}^{\infty} \frac{e^{-ik\xi}\,d\xi}{(x-\xi)} + \pi k\Gamma e^{-ikx}\,W(k,h,m)\right]$$

where

$$W(k,h,m) = \frac{1 + \sum_{q=1}^{Q-1}\left(e^{khQ}e^{i2\pi m}\right)^{(Q-q)/Q} e^{i\psi_q}}{e^{khQ}e^{i2\pi m} - 1}$$

The function W(k,h,m) may be thought of as a weighting function for the vorticity shed by previous blades or in previous revolutions.

This form of the downwash equation can be solved by applying Söhngen's inversion formula [11]. Satisfying the condition *f(1)* = finite is the same as employing the Kutta condition; thus the bound vorticity is

$$\gamma_a(x) = \frac{2}{\pi}\sqrt{\frac{1-x}{1+x}}\left[\int_{-1}^{1}\sqrt{\frac{1+\xi}{1-\xi}}\,\frac{w(\xi)\,d\xi}{x-\xi} - \frac{ik\Gamma}{2\pi}\int_{-1}^{1}\sqrt{\frac{1+\xi}{1-\xi}}\left(\frac{1}{x-\xi}\right)\int_{1}^{\infty}\frac{e^{-ik\eta}\,d\eta}{\xi-\eta}\,d\xi + \frac{k\Gamma}{2}W(k,h,m)\int_{-1}^{1}\sqrt{\frac{1+\xi}{1-\xi}}\,\frac{e^{-ik\xi}\,d\xi}{x-\xi}\right]$$

Evaluating the circulation over the entire airfoil yields

$$\Gamma = e^{ik}\int_{-1}^{1}\gamma_a(x)\,dx = \frac{2\int_{-1}^{1}\sqrt{\frac{1+\xi}{1-\xi}}\,w(\xi)\,d\xi}{i\pi k\left[\frac{1}{2}\left(H_1^{(2)} + iH_0^{(2)}\right) + \left(J_1 + iJ_0\right)W(k,h,m)\right]}$$

where the Hankel and Bessel functions are evaluated at reduced frequency, k.

Since the airfoil has been replaced by a vortex sheet and when simple harmonic motion is assumed, the generalized Bernoulli equation becomes

$$\Delta p(x) = -\rho\left[V\gamma_a(x,t) + i\omega b\int_{1}^{x}\gamma_a(\xi,t)\,d\xi\right]$$

Substituting the bound vorticity equation and the airfoil circulation equation into the generalized Bernoulli equation yields

$$-\frac{\Delta p(x)}{\rho V} = \frac{\frac{2i}{\pi}\left[H_0^{(2)} + 2J_0 W(k,h,m)\right]}{H_1^{(2)} + iH_0^{(2)} + 2\left[J_1 + iJ_0\right]W(k,h,m)}\int_{-1}^{1}\sqrt{\frac{1-x}{1+x}}\sqrt{\frac{1+\xi}{1-\xi}}\,w(\xi)\,d\xi + \frac{2}{\pi}\int_{-1}^{1}\left[\sqrt{\frac{1-x}{1+x}}\sqrt{\frac{1+\xi}{1-\xi}}\left(\frac{1}{x-\xi}\right) - \frac{ik}{2}\log\left(\frac{1-x\xi-\sqrt{1-x^2}\sqrt{1-\xi^2}}{1-x\xi+\sqrt{1-x^2}\sqrt{1-\xi^2}}\right)\right]w(\xi)\,d\xi$$

This pressure distribution has the same form as Theodorsen if the factor multiplying the first integral is written as

$$\frac{2}{\pi}\left[1 - C'(k,h,m)\right]$$

where C'(k,h,m) is Loewy's lift deficiency function. Solving for C'(k,h,m) yields

$$C'(k,h,m) = \frac{H_1^{(2)} + 2J_1 W(k,h,m)}{H_1^{(2)} + iH_0^{(2)} + 2\left[J_1 + iJ_0\right] W(k,h,m)}$$

where the Hankel and Bessel functions are evaluated at reduced frequency, k. Since C'(k,h,m) is not a function of location along the airfoil, the integration of the pressure distribution will yield force and moment equations identical to Theodorsen except C(k) will be replaced by C'(k,h,m). It is clear that as W(k,h,m) approaches zero, $\mathbf{C'(k,h,m) = C(k)}$, and this corresponds to an infinite wake spacing ($h \to \infty$).

Since the wake weighting function is periodic in nature, Loewy [5] shows that the wake weighting function for a multi-blade rotor can be expressed by a single-blade rotor with modified values of h and m that yield the same value of W. For a single-blade rotor, the wake weighting function becomes,

$$W(k,h,m) = \frac{1}{e^{kh}e^{i2\pi m} - 1}$$

where h and m are the modified values of wake spacing and frequency ratio respectively. For the case of the single-blade rotor the wake weighting function can be separated into its real and imaginary parts, $\mathbf{W(k,h,m) = \hat{\alpha} + i\hat{\beta}}$, where

$$\hat{\alpha} = \frac{\cos 2\pi m - e^{-kh}}{e^{kh} - 2\cos 2\pi m + e^{-kh}}$$

and

$$\hat{\beta} = \frac{-\sin 2\pi m}{e^{kh} - 2\cos 2\pi m + e^{-kh}}$$

The lift deficiency function can also be separated into its real and imaginary part $\mathbf{C'(k,h,m) = F' + iG'}$, where

$$F' = \frac{J_1(1+2\hat{\alpha})A - (Y_1 - 2J_1\hat{\beta})B}{A^2 + B^2}$$

$$G' = -\frac{(Y_1 - 2J_1\hat{\beta})A + J_1(1+2\hat{\alpha})B}{A^2 + B^2}$$

and

$$A = J_1(1+2\hat{\alpha}) + Y_0 - 2J_0\hat{\beta}$$

$$B = -Y_1 + 2J_1\hat{\beta} + J_0(1+2\hat{\alpha})$$

(This is equivalent to Loewy's equations [5] when the substitutions $\alpha = 1 + 2\hat{\alpha}$ and $\beta = -2\hat{\beta}$ are used.) Plots of Loewy's lift deficiency function are shown in Figures 9 through 12. It is easily seen that there are rapid changes in the lift deficiency function as k, h, and m vary.

Since Loewy's lift deficiency function is completely analogous to Theodorsen's lift deficiency function, the propulsive force determined by Garrick [2] in pure plunge can be calculated for the rotary-wing case by

$$P_x = \pi \rho b \omega^2 h_o^2 \left[(F')^2 + (G')^2 \right]$$

Defining a propulsive force coefficient as

$$C_{P_x} = \frac{P_x}{\frac{1}{2}\rho v^2 (2b)} = \pi k^2 \bar{h}_o^2 \left[(F')^2 + (G')^2 \right]$$

where $\bar{h}_o$ is the amplitude of deflection non-dimensionalized by semi-chord. This makes the propulsive force coefficient analogous to a negative drag coefficient. A plot of propulsive force coefficient in pure plunge and pure pitch as a function of frequency ratio for k = 0.1234 are shown in Figure 13 and 14. It can be seen that C_{P_x} is reasonably constant for $0.15 < m < 0.8$ and greater that the "Katzmayr effect" ($h \to \infty$). For $m < 0.15$ and $m > 0.8$, C_{P_x} begins to decrease to the point where it eventually becomes less than the "Katzmayr effect."

Finite Wake Lift Deficiency Function

Loewy's theory can be extended to the case of a finite number of wakes below the rotor blade by modifying the wake weighting function. This modified wake weighting function is completely interchangeable with Loewy which makes the definition of the lift deficiency function the same, but with $\hat{\alpha}$ and $\hat{\beta}$ modified by the new wake weighting function. Since the lift deficiency function is of the same form, the aerodynamic forces and moments will be the same, but with a modified lift deficiency function. Loewy has already shown that the rotary-wing problem reduces to the case of a single rotor. The modified wake weighting function will also be developed for the case of the multi-blade rotor, and then reduced to the case of the single-blade rotor with modified wake spacing and frequency ratio.

The development of a finite wake lift deficiency function is the same as Loewy [5] as described earlier. The integral downwash equation for a finite number (N) of revolutions is

$$\begin{aligned} w(x) = -\frac{1}{2\pi}\Bigg[& \int_{-1}^{1} \frac{\gamma_a(\xi)d\xi}{x-\xi} - ik\Gamma \int_{1}^{\infty} \frac{e^{-ik\xi}d\xi}{x-\xi} \\ & - ik\Gamma \sum_{q=1}^{Q-1} e^{-i(2\pi mq/Q - \psi_q)} \sum_{n=0}^{N} e^{-i2\pi mn} \int_{-\infty}^{\infty} \frac{e^{-ik\xi}(x-\xi)d\xi}{(x-\xi)^2 + (nQ+q)^2 h^2} \\ & - ik\Gamma \sum_{n=1}^{N} e^{-i2\pi mn} \int_{-\infty}^{\infty} \frac{e^{-ik\xi}(x-\xi)d\xi}{(x-\xi)^2 + n^2 Q^2 h^2} \Bigg] \end{aligned}$$

where the summations to infinity have been replaced by finite sums to *N*. Solving the last two integrals in the same manner as Loewy result in

$$\begin{aligned} w(x) = -\frac{1}{2\pi}\Bigg[& \int_{-1}^{1} \frac{\gamma_a(\xi)d\xi}{x-\xi} - ik\Gamma \int_{1}^{\infty} \frac{e^{-ik\xi}d\xi}{x-\xi} \\ & + \pi k\Gamma e^{-ikx} \Bigg(\sum_{q=1}^{Q-1} e^{-i(2\pi mq/Q - \psi_q)} \sum_{n=0}^{N} e^{-i2\pi mn} e^{-k(nQ+q)h} \\ & + \sum_{n=1}^{N} e^{-i2\pi mn} e^{-nQkh} \Bigg) \Bigg] \end{aligned}$$

Since this is in the same form as the case of an infinite number of revolutions, the terms enclosed by the parentheses can be defined as the finite wake weighting function, or

$$W_N(k,h,m) = \sum_{q=1}^{Q-1} e^{-i(2\pi mq/Q - \psi_q)} \sum_{n=0}^{N} e^{-i2\pi mn} e^{-k(nQ+q)h} + \sum_{n=1}^{N} e^{-i2\pi mn} e^{-nQh}$$

It is easily seen that this modified wake weighting function is periodic once the relationship ψ_q is known, and a multi-blade rotor can be reduced to a single-blade rotor with modified wake spacing and frequency ratio. For the case of

the single-blade rotor (Q = 1),

$$W_N(k,h,m) = \sum_{n=1}^{N} e^{-i2\pi mn} e^{-nkh}$$

It can be shown that as N→∞, this becomes a convergent geometric series which reduces to Loewy's wake weighting function.

The solution to the remainder of the finite wake problem is identical to Loewy, but with a modified finite wake lift deficiency function. To keep the finite wake lift deficiency function separate from it is defined as follows:

$$C^*(k,h,m) = \frac{H_1^{(2)} + 2J_1 W_N}{H_1^{(2)} + iH_0^{(2)} + 2\left[J_1 + iJ_0\right] W_N}$$

Separating the finite wake weighting function is separated into real and imaginary parts, $\mathbf{W}_N = \hat{\alpha}_N + \mathbf{i}\hat{\beta}_N$, where

$$\hat{\alpha}_N = \sum_{n=1}^{N} e^{-nkh} \cos 2\pi mn$$

$$\hat{\beta}_N = \sum_{n=1}^{N} \left(-e^{-nkh} \sin 2\pi mn\right)$$

The finite wake lift deficiency function becomes $\mathbf{C}^* = \mathbf{F}^* + \mathbf{iG}^*$, where

$$F^* = \frac{J_1(1+2\hat{\alpha}_N)A_N - (Y_1 - 2J_1\hat{\beta}_N)B_N}{A_N^2 + B_N^2}$$

$$G^* = -\frac{(Y_1 - 2J_1\hat{\beta}_N)A_N + J_1(1+2\hat{\alpha}_N)B_N}{A_N^2 + B_N^2}$$

and

$$A_N = J_1(1+2\hat{\alpha}_N) + Y_0 - 2J_0\hat{\beta}_N$$

$$B_N = -Y_1 + 2J_1\hat{\beta}_N + J_0(1+2\hat{\alpha}_N)$$

Single Wake Case

For the case of a single wake, the wake weighting function reduces to

$$W_1 = e^{-(i2\pi m + kh)}$$

and

$$\hat{\alpha}_1 = e^{-kh}\cos 2\pi m$$

$$\hat{\beta}_1 = -e^{-kh}\sin 2\pi m$$

Plots of the single wake lift deficiency function are shown in Figures 15 through 18. The propulsive force can be calculated by replacing F(k) and G(k) in Garrick's equations with F^* and G^*. A plot of the propulsive force coefficient in pure plunge and pure pitch as a function of frequency ratio for k = 0.1234 are shown in Figures 19 and 20. It is interesting to note that for $0.24 < m < 0.7$ the propulsive force is greater than the "Katzmayr effect" with the maximum occurring just prior to m = 0.5. The maximum propulsive force for a single wake is greater than the infinite number of wakes. The reason for this increase is that F and F′ are never greater than 1.0, but F^* as m approaches 0.5 exceeds 1.0.

When m = 0.5, this corresponds to the wakes being 180° out of phase, and the vortex from the wake of the reference blade in the current revolution is directly above an oppositely spinning vortex from the single wake of the previous blade or revolution. This efficient use of the vortices in the wake causes F^* to exceed 1.0. As the number of wakes increases the vortices from lower wakes are not always 180° out of phase with the first wake. When m = 0.5, each wake is 180° out of phase with the wake above and below it. Thus, each wake is in phase with the wakes ±2 wake spacings from it. Figures 19 and 20 show that when m = 0, the propulsive force is substantially reduced, but since the wake spacing is greater than that of the previous wake, the effect of the in-phase wake is not as strong. As the wake spacing increases this effect diminishes.

NPS Unsteady Panel Code

This code was written by Pang [12] to solve the potential flow for two airfoils executing unsteady motions in an inviscid,incompressible flow. This code is an extension of the single airfoil code [13]. In the past, a number of investigators have solved the steady flow problem using source and vortex paneling, the most prominent ones being Hess and Smith [14]. A few others have extended this approach to the case of unsteady motion of single airfoil, notably Basu and Hancock [15] and Kim and Mook [16].

In this code, the two airfoil surfaces are approximated by a large number of surface elements and a uniform source distribution and a uniform vorticity are placed on each element. The source strength varies from element to element, while the vortex strength is the same for all elements. The singularity strengths are determined from the flow tangency condition on both airfoil surfaces and the two Kutta conditions at both trailing edges.

The unsteady flow problem is similar to the steady one in that they both have the same governing equation, Laplace equation, and that for both problems, the pressure and velocity calculations can be computed separately and consecutively. The unsteady flow problem differs from the steady one in that the continuous shedding of vorticity into the trailing wake needs to be included in the computation. According to the vorticity conservation theorem any change in circulation around the airfoil must be matched by an equal and opposite vortex shed from the airfoil trailing edge. The presence of the counter vortices provide the flow with a kind of memory in that the flow at a particular time is affected by the bound circulation of the past. It is this nonlinearity that distinguishes the numerical technique required for the unsteady flow solution from the simple steady one. The present approach follows closely the original panel method of Hess and Smith, while with regard to the modelling of the wake it adopts the procedure advocated by Basu and Hancock.

A uniform source distribution and a uniform vorticity distribution is placed on each panel at time t. The wake consists of a single vorticity panel attached as an additional element on each airfoil through which the vortices are shed into the respective wake as a series of point vortices which are being convected downstream with the fluid. This panel is farther characterized by its length and its inclination with respect to the local frame of reference. After each time step, the vorticity of the wake panel is concentrated into a single point vortex and convected downstream. Simultaneously a new wake panel is formed. The downstream wake of point vortices is thus formed by the shed vorticity of previous time steps. The computed thrust coefficients (negative drag) presented by Platzer et al [6] using the panel code showed good agreement with the results obtained by Bosch [17].

Extensive comparisons with Theodorsen have been done by Riester [18]. The code results show a very good agreement with the flat plate theory (Theodorsen) as shown in Fig. (29) through (31), which compare the real,

imaginary, and the magnitude of the lift coefficients versus reduced frequency k. Also, shown in Fig. (32), is the average drag coefficient versus the amplitude of oscillation, hbar, for k=.05. Results were compared with Garrick and it showed very good agreement at small amplitudes of vertical oscillation.

5. DISCUSSION OF RESULTS

The Physics of an Airfoil Oscillating in Plunge

Consider the case of an isolated airfoil oscillating in plunge, without the presence of adjacent wakes. This is the case where the resulting drag force is a propulsive force. It is the classic "Katzmayr effect" case. It is also the main case considered by Garrick [2]. We can understand the physics of this case by modeling it in any of three ways. These are:

(a) By the unsteady aerodynamic theory of Theodorsen for a plunging airfoil.

(b) By the unsteady aerodynamic theory of Loewy for a plunging airfoil, where wake spacing is taken as infinite.

(c) By the "NPS Unsteady Panel Code" (UPC) either without the wake, or for the case where the wake spacing is taken as very large.

The advantage of the "NPS Unsteady Panel Code" is that it provides us with better graphics by which to understand the problem. That is, it gives time history plots of wake position, as well as lift and drag. But in using it we must be very careful, if we plan to compare results with closed form solutions such as those of Theodorsen's and Loewy's. We must remember that the closed form solutions are based upon a very thin flat plate airfoil undergoing very small motions when we model it in the unsteady panel code.

Figure 21 shows the results from the unsteady panel code. For the calculations NACA 0007 airfoil was selected, set at zero degrees mean angle of attack. Reduced frequency was k = .0617. Non-dimensional wake spacing was for h = 200 (mathematically equivalent to infinite spacing). Amplitude of plunge oscillation was $\Delta h = \pm 0.14$.

Shown in Figure 21(a) is the wake positioning for h=200 (wake at infinity). Plotted in Figure 21(b) is the time history of lift variation, C_l, and plotted in Figure 21(c) is the time history of drag variation, C_d. Study of the figure reveals the following. We observe from Figure 21(b) that the lift varies as the frequency of oscillation, with a mean lift value of zero as we would expect. Amplitude of oscillatory lift is $C_l = \pm 0.0510$.

Figure 21(b) clearly shows the "Katzmayr effect". We note that the calculated drag varies at twice the plunge oscillation frequency of the airfoil. Also, observe that the airfoil is generating a propulsive force as indicated by the mean value of drag, which is seen to have a negative value. From the computer printout, the amplitude of drag is seen to vary from $C_d = - 0.000392$ to $C_d = + 0.00000$, for a mean propulsive force, $C_d = - 0.000196$.

Oscillations in Plunge with Wake Effects

Figures 22, 23, and 24 consider the same case as above, that of an airfoil oscillating in plunge, but with the introduction of a wake layer in the near proximity of the reference airfoil. That is we now position the wake at h = 2 and consider three cases of the frequency ratio, m. The cases selected are for m = 0.0, m = 0.2083, and m = 0.50. These correspond to phase angles of 0°, 75°, and 180°, respectively.

It should be noted that the phase angles relate to the phase relationship between the reference airfoil and the wake layer of shed vorticity. These phase angles are achieved in the panel code by establishing the proper time phase between the initiation of the wake vorticity and the oscillations of the reference airfoil. This time phase is in turn a function of the frequency of oscillation which is directly related to k, reduced frequency.

For the results presented here for k = .0617, this corresponds to 50.92 time units for m = 0.0 (0° phase); 61.53 time units for m = 0.2083 (75° phase); and 76.38 time units for m = 0.50 (180° phase), etc.. If "k" changes, this corresponds to a change in frequency. For results shown in the paper for k = .1234, this corresponds to 50.92 time units for m = 0.0 (0° phase); 56.23 time units for m = 0.2083 (75° phase); and 63.65 time units for m = 0.50 (180° phase), etc..

Wake at Zero Degree Phase: Shown in Figure 22(a) is the wake positioning for m = 0.0, the case where the wake shed from the second airfoil at h=2 is in phase with the wake shed from the reference airfoil itself. Figure 22(b) shows the time history of lift variation on the reference airfoil. This is indicated by the solid line for Cl_1.

The dashed line, Cl_2, indicates the variation of lift on a second airfoil located at the point of initiation of the wake layer at h = 2. Since the upstream effect of the vorticity shed from the reference airfoil is quite small, the results for airfoil are similar to those of Figure 21, where the wake layer is at infinity. Our discussion will focus on $airfoil_1$, indicated by the solid line.

In Figure 22(b), the interesting part of the time history starts 50.92 time units into the plot. Figure 22(a) shows it takes this amount of time until the rotor wake reaches the reference airfoil. We can make two findings with respect to the lift time history results shown. First, as would be expected for an airfoil oscillating about zero angle of attack, the mean lift is zero. Second, comparing with Figure 21, we find that while the mean lift is zero, the amplitude of lift oscillation is less in the presence of the wake at m = 0.0 phasing. The decrease in amplitude being 1 - .0430/.0510 or 15.7%.

Figure 22(c) shows the effect of the wake vorticity at h = 2 on the drag time history of the reference $airfoil_1$. We first note the doubling of frequency that is characteristic of plunge oscillations. Recall that in the case of Figure 21 where we considered plunge oscillations without the influence of a layer of wake vorticity that we found C_d = - 0.000196 propulsive force. In this case we find from the computer printout that the amplitude of drag varies from Cd_1 = - 0.000278 to Cd_1 = + 0.00000, for a mean propulsive force, Cd_1 = - 0.000139. We conclude that the effect of the wake vorticity at phasing m = 0.0 is to reduce the "Katzmayr effect". The amount of reduction is (.000196 - .000139)/.000196 or 29.1%.

Wake at 75 Degrees Phase: For this case which is presented in Figure 23, m equals 0.2083. The wake pattern is depicted in Figure 23(a) where it is seen that after 61.53 time units, the wake vorticity will be positioned directly beneath the reference airfoil. The time history of lift is given in Figure 23(b). Comparison of oscillatory lift values with those of Figure 21 (no wake) shows they are identical, since the values at 75 degrees phase are the same as that for infinite wake. That is, Cl_1 varies about zero angle attack at an amplitude of $\pm$ 0.0510. This corresponds to the same oscillatory amplitude (versus "Katzmayr" effect - infinite wake spacing) of .0510/.0510 or unity.

The time history of drag is seen to vary at twice the plunge oscillation frequency of the airfoil. We also observe that the airfoil is generating a propulsive force as indicated by the mean value of drag, which is seen to have a negative value. The computer printout shows a variation of drag is seen to very from Cd = -.000392 to Cd = +0.0000, for a mean value of Cd = -0.000196. The reader will note these results are identical to the "no wake" case discussed earlier.

Results of this research confirm that there is a phase angle, m, at which the effect of the wake vorticity on the reference airfoil gives the same results as when the wake is removed (located at infinity). It has been shown at a phase angle of zero degrees that the shed wake vorticity increases the drag on the oscillating reference airfoil, i.e. diminishes the "Katzmayr" effect. Conversely we will find that at a phase angle of about 180 degrees, there is a significant decrease in drag at the reference airfoil due to the wake vorticity. This implies an intermediate phase angle at which the drag is identical to the "Katzmayr" effect. It turns out that such a phase angle exists. In fact, at this phase angle the lift, drag and pitching moment are found to be identical to the case of no wake, and match the "no wake" values identically. The phase angle at which this occurs is 75° or m = 0.20833, for the case considered here.

Wake at 180 Degrees Phase: So far we have found in the case of the plunging airfoil that the wake at zero degrees phase attenuates the "Katzmayr" propulsive force, while the wake at seventy-five degree phase gives us close results to the "no wake at all" case. Based on these findings we would expect the wake at 180° phase (m = 0.5) to enhance the propulsive force.

Figure 24(a) shows the wake pattern for this case. The proper phasing is achieved by positioning the reference airfoil 76.38 time units to the right of the second airfoil, the airfoil that generates the wake. The time history of lift given in Figure 24(b) shows that with this wake phasing the amplitude of lift is enhanced. ***While the mean lift remains zero as expected, the oscillatory amplitude increases by 0.0590/0.0510 - 1. or +15.7%.***

The corresponding effect on propulsive force is shown in the time history given by Figure 24(c). The computer printout shows an amplitude variation in the drag values varying from Cd_1 = - 0.000522 to Cd_1 = + 0.000002, for

a mean propulsive force, Cd_1 = - 0.000262. ***This represents an enhancement of the "Katzmayr" propulsive force of .000262 - .000196/.000196 or 33.7%.*** It should be recognized that this enhancement has been obtained by simply considering one layer of wake vorticity at an arbitrary positioning with respect to the reference airfoil. No effort has been made here to further optimize the enhancement. This is recommended for future investigations.

Wake for Phase Angles from 0° to 360°: It is of interest next to explore the complete range of phase angles of one layer of wake vorticity, and these results are shown in Figure 25. The circles in Figure 25 denote the calculated values of propulsive force for the plunging airfoil for the range of phase angles from 0° to 360°, as determined by the NPS unsteady panel code. Superimposed on the plot of Figure 25 are the analytical closed form results of the Loewy theory as modified for one wake, as previously shown in Figure 19. Note the good agreement between the two sets of results. It is likely that the agreement can be further improved by increasing the number of panels from 100, used for the calculations here, to 150 or 200.

The Case of an Airfoil Oscillating in Pitch

As was done previously for an airfoil oscillating in plunge, we will now consider the case of an airfoil oscillating in pitch with particular emphasis on drag or propulsive force. We will first look at the case without the presence of layers of adjacent wake, then look at the wake effect including the important consideration of phasing. We will begin by considering numerical results and then study closed form solutions. We consider initially the "NPS Unsteady Panel Code"[6] and then compare these results with Theodorsen's [4] and Loewy's [5] theory.

In the interest of space limitations, the figures have not been included. We review the results from the unsteady panel code. Considered is the case of an NACA 0007 airfoil set at zero degree mean angle of attack. The airfoil is oscillating with an amplitude of $\Delta\alpha = \pm$ 1 degree. The reduced frequency is taken at k = .0617 and the non-dimensional wake spacing was for h = 200, which is numerically equivalent to having the wake at infinity.

The time history of lift variation, C_l, and the time history of drag variation, C_d. reveal the following. We observe that the lift varies as the frequency of oscillation, with a mean lift value of zero as we would expect. In contrast to the lift time history, the drag time history indicates that the calculated drag varies at twice the frequency of the pitch oscillation. The amplitude is given by $\Delta C_d = \pm$ 0.000192. The mean drag value is found to be C_d = 0.000090 and the mean lift is of course 0.0 at zero degrees angle of attack.

Oscillations in Pitch with Wake Effects

Now consider the same case as above, that of an airfoil oscillating in pitch, but with the introduction of a wake layer in the near proximity of the reference airfoil. That is, we now position the wake at wake spacing, h = 2, and consider three cases of the frequency ratio, m. The cases selected are for m =0.0, m = 0.2083, and m = 0.50. These correspond to phase angles of 0°, 75°, and 180°, respectively.

Wake at Zero Degree Phase: This is the case where the wake below the airfoil at h = 2 is in phase with the wake shed from the reference airfoil itself. Review of the results indicates a reduction in the amplitude of lift variation for the m = 0.0 case when compared to the case with no wake at all (or wake at infinity). We find a change in amplitude from $Cl_1 = \pm$ 0.103 (infinite wake) to $Cl_1 = \pm$ 0.087, for a decrease of 16.5%. We also find that an increase in mean steady drag accompanies the reduction in lift amplitude of Figure 16(b), for the m = 0.0 case. For the wake at infinity, the mean Cd_1 = 0.000090, whereas for the wake with m = 0.0 phasing the mean Cd_1=0.000186, representing a drag increase of ΔCd_1 = 0.000096, or 206.7%.

Wake at 75 Degrees Phase: This is the case when m equals 0.2083. The time history of lift indicates that the amplitude of lift variation is $\Delta C_l = \pm$ 0.103 versus $\pm$ 0.103 for the wake at infinity. From review of the results, we find the following. From the computer printout the drag varies from Cd_1 = - 0.0.000103 to Cd_1 = 0.0.000282, which gives a mean drag value Cd_1 = + 0.000089. Amplitude of drag oscillation is found to be $\Delta Cd_1 = \pm$0.000192. Recall the infinite wake case gave a mean drag value of Cd_1 = 0.000090 with an amplitude of drag oscillation ΔCd1 = $\pm$ 0.000192. Thus for the case of pure pitch, similar to pure plunge, the oscillatory and mean values of lift and drag are identical for the infinite wake case and then when m = .2083, or 75° wake phasing

Wake at 180 Degrees Phase: The case of 180°-wake phasing for an airfoil oscillating in pitch is now considered. Proper phasing is achieved by positioning $airfoil_1$ 76.38 time units to the right of $airfoil_2$, where the second airfoil is the hypothetical airfoil that generates the wake. At 180°-phase angle, we find we achieve lift enhancement in this case

of pure pitch, similar to what we found in plunge. ***While the mean lift remains zero as expected, the oscillatory amplitude increases by 0.120/0.103 - 1. or 16.5%. This is about the same increase in oscillatory lift achieved in the plunge case (15.6%).***

The corresponding effect on drag force is as follows. The computer printout shows an amplitude variation in the drag values ranging from Cd_i = -0.000273 (propulsive force) to Cd_i = + 0.000173 (drag). This gives a mean drag value of Cd_i = - 0.000050 (propulsive force) with a oscillatory amplitude of $\Delta Cd_i = \pm$ 0.000223. Similar to the plunge case, ***this represents a drag reduction of 100% plus addition of propulsive force of 0.000050/0.000090, or 55.5% of the original drag value***

Wake for Phase Angles from 0° to 180°: It is of interest next to examine the range of phase angles from 0° to 180° (m = 0.0 to 0.5) and their effect on airfoil drag for the case of pure pitch for k = .0617 and k = .1234. These values are plotted in Figure 28.

6. CONCLUSIONS

Certain conclusions can be drawn from these results. As related to unsteady aerodynamics in general, these are:

1. For drag, in both cases of pure plunge and pure pitch, wake phasing can increase or decrease the steady component of drag acting on the airfoil. The increase in the steady component of propulsive force due to wake phasing in the case of pure plunge was sufficient to significantly enhance the "Katzmayr" effect value of propulsive force. Whereas in the case of pure pitch, the reduction in steady drag obtained by optimum wake phasing was sufficient to reduce the steady drag to zero and in addition provide some amount of propulsive force.

2. For an airfoil oscillating in plunge or pitch, for optimum reduction in drag and enhancement of vibratory lift, the phase angle of the wake vorticity in the single wake case with respect to motion of the reference airfoil should be about 180°.

3. For an airfoil oscillating in plunge or pitch, the largest value of steady drag and smallest value of oscillatory lift occurs when the phase angle of the wake vorticity with respect to motion of the reference airfoil is about 0°.

4. For lift, in both pure plunge and pure pitch in the single wake case, wake phasing can increase or reduce the oscillatory lift acting on the airfoil. Whereas in the absence of wake vorticity, the effect of oscillations decreases the lift (lift deficiency). With the wake present we also observe lift enhancement (lift efficiency).

5. There exists a phase angle, 75° for the panel code case studied here (k = .0617, h = 2) where the effect of the wake vorticity on the reference airfoil is identical to the case of the wake at infinity (h = 200), or no wake vorticity at all. The significance of this finding is that it shows that a wake layer (h = 2) at a certain phase angle will result in the same flow field about the reference airfoil in terms of both oscillatory and steady lift and drag, as that for no wake layer (or the wake layer located at infinity, h = 200).

As related to the NASA-Army HHC flight test program for the OH-6A helicopter reported here and in references [1] and [3]:

1. The reductions in main rotor shaft torque and engine torque power presented in this paper are feasible when evaluated with reference to the "Katzmayr effect" and the associated additional drag reduction that can be achieved in both pitch and plunge due to wake phasing.

2. As a corollary to this finding, we observe in Figure 6 that HHC has the least effect on rotor and engine power at the highest airspeed tested, 100 knots. At this airspeed the wake is transported furthest from the rotor disk due to the component of forward velocity acting through the disk, the disk being at a higher angle of attack. From the results of this paper, the increased wake spacing diminishes the effect of drag enhancement.

3. As a second corollary, we observe that the "closure or repeatability" of OH-6A open loop performance results at 0° controller phase is relatively poor (Figs. 4, 5, and 6) when compared with open loop vibration results from the same flights and at the same airspeeds reported in Ref. [1] (See Figs. 13, 15, and 17 of that reference). A possible explanation on the basis of these findings is the sensitivity of OH-6A power levels ("HHC on") to wake position and the difficulty of repeating wake position during flight testing.

7. REFERENCES

1. E. R. Wood, R. W. Powers, J. H. Cline, and C. E. Hammond, "On Developing and Flight Testing a Higher Harmonic Control System", *Journal of the American Helicopter Society*, Vol. 30, n° 2, Jan. 1985.

2. I. E. Garrick, "Propulsion of a Flapping and Oscillating Airfoil, *NACA T.R. n°* 567, 1936.

3. E. R. Wood, J. Higman, and R. Kolar, "Higher Harmonic Control Promises Improved Dynamic Interface Operations", AGARD Proceedings of the 78th Flight Mechanics Panel, May 20-23, 1991, Seville, Spain.

4. T. Theodorsen, "General Theory of Aerodynamic Instability and the Mechanism of Flutter", *NACA T.R. n°* 496, 1935.

5. R. G. Loewy, "A Two-Dimensional Approximation to the Unsteady Aerodynamics of Rotary Wings", *Journal of the Aeronautical Sciences*, Vol. 24, n° 2, Feb. 1957.

6. M. F. Platzer, K. S. Neace, and C. K. Pang, "Aerodynamic Analysis of Flapping Wing Propulsion", *AIAA Paper n°* 93-0484, 31st Aerospace Sciences Meeting, Reno, NV, January 11-14, 1993.

7. R. Katzmayr, "Effect of Periodic Changes of Angles of Attack on Behavior of Airfoils", *NACA T.M. n°* 147, Oct. 1922.

8. E. G. Richardson, "The Physical Aspects of Fish Locomotion", *Journal of Experimental Biology*, Vol. III, n° 1, pp. 63-74, 1936.

9. Th. von Karman, and J. M. Burgers, "General Aerodynamic Theory-Perfect Fluids", Aerodynamic Theory, W. F. Durand, ed., Vol. II, Julius Springer (Berlin), 1935.

10. R. H. Scanlan, and R. Rosenbaum, Introduction to the Study of Aircraft Vibration and Flutter, The MacMillan Company, New York, 1962.

11. H. Söhngen, "Die Losungen der Integralgleichung und deren Anwendung in der Tragflugeltheorie", Mathematische Zeitschrift, Band 45, 1939.

12. K. C. Pang , "A Computer Code (USPOTF2) for Unsteady Incompressible Flow Past Two Airfoils." Master's Thesis Naval Postgraduate School, Monterey California, Sep. 1988 pp. 1-156.

13. H. N. Teng, "The Development of a Computer Code (U2DIIF) for the Numerical Solution of Unsteady, Incompressible Flow Over an Airfoil. " Master's Thesis, Naval Postgraduate School, Monterey California, Jun. 1987, pp. 1-135.

14. J. L. Hess, and A. M. O. Smith,"Calculation of Potential Flow about Arbitrary Bodies." Progress in Aeronautical Sciences, Vol. n° 8, pp. 1-138, Pergamon Press, Oxford, 1966.

15. B. C. Basu, and G. J. HanChock,"The Unsteady Motion of a Two-Dimensional Airfoil in Incompressible Inviscid Flow." J. Fluid Mechanics , Vol. n° 87 , pp. 159-168 ,1978.

16. M. J. Kim, and D. T. Mook,"Application of Continuous Vorticity Panels to General Unsteady Incompressible Two-Dimensional Lifting Flows." Journal of Aircraft , Vol. 23 ,n°. 6 ,pp. 464-471, 1986.

17. H. Bosch,"Interfering Airfoils in Two-Dimensional Unsteady Incompressible Flow." AGARD CP-227 ,Paper n°. 7 & ,Sep. 1977.

18. P. J. Riester, " A Computational and Experimental Investigation of Incompressible Oscillatory Airfoil Flow and Flutter Problems." Master's Thesis Naval Postgraduate School, Monterey California, June 1993.

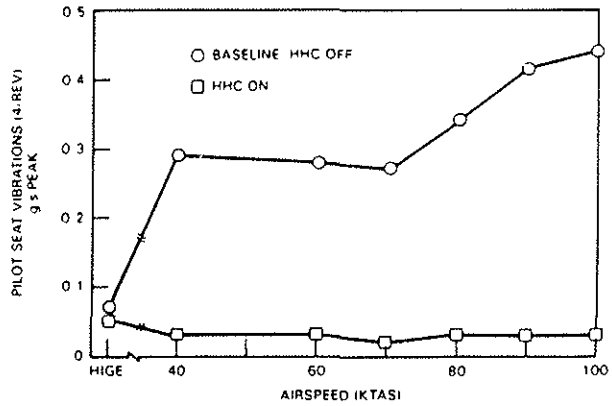

Fig. 1 Comparison of 4P vertical vibrations at pilot seat versus airspeed with HHC "on" and "off".

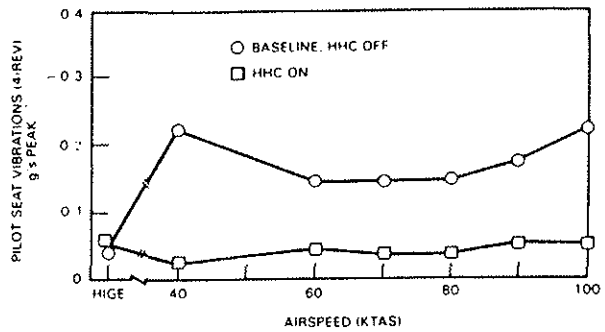

Fig. 2 Comparison of 4P lateral vibrations at pilot seat versus airspeed with HHC "on and "off".

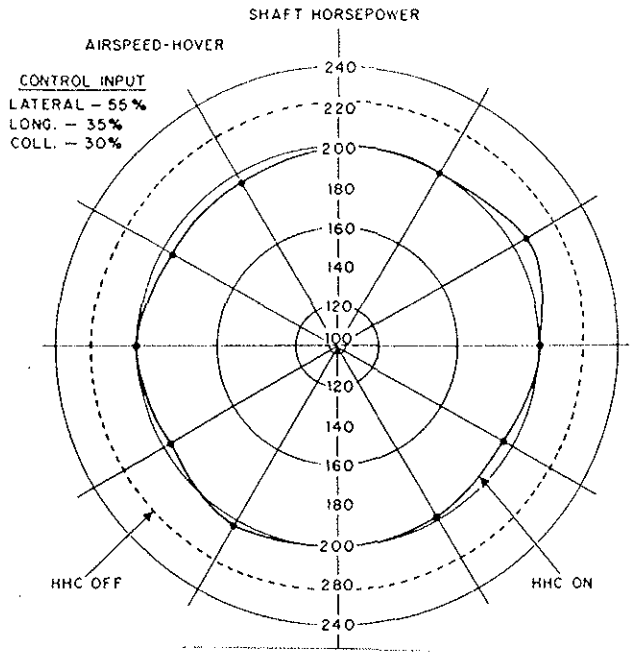

Fig. 3(a) Effect of HHC on main rotor shaft power in hover for selected set of open loop inputs.

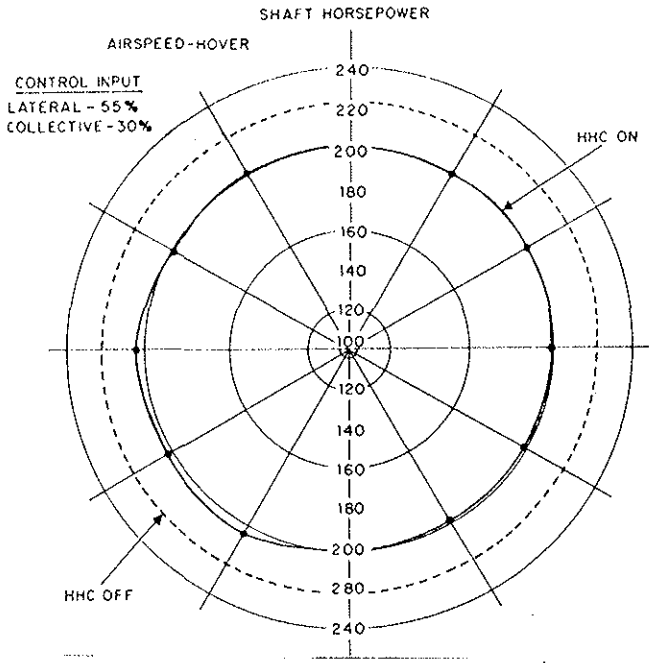

Fig. 3(b) Effect of HHC on main rotor shaft power in hover for selected set of open loop inputs.

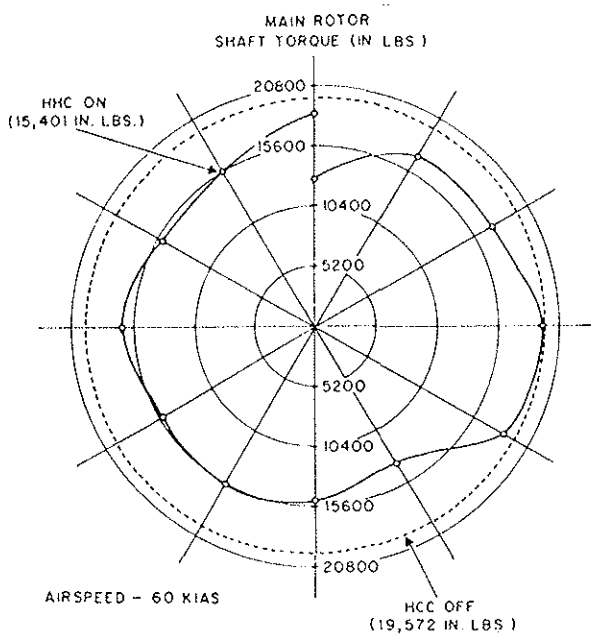

Fig. 4(a) Effect of HHC on main rotor shaft torque at 60 KIAS for lateral input of ± 0.33 degrees.

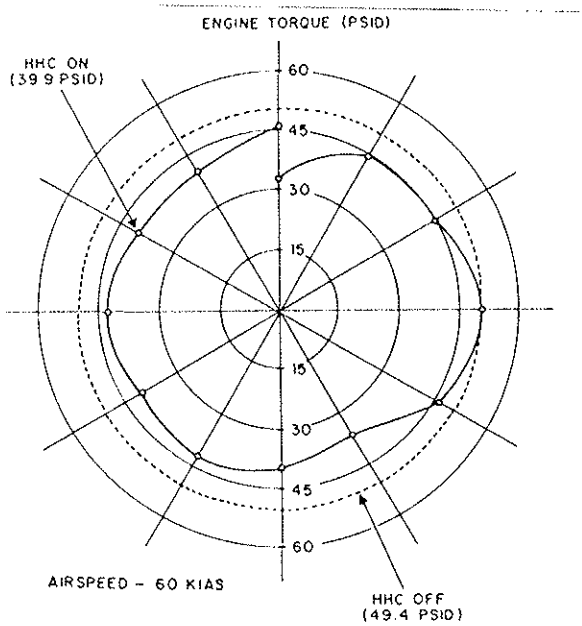

Fig. 4(b) Effect of HHC on engine torque pressure at 60 KIAS for lateral input of ± 0.33 degrees.

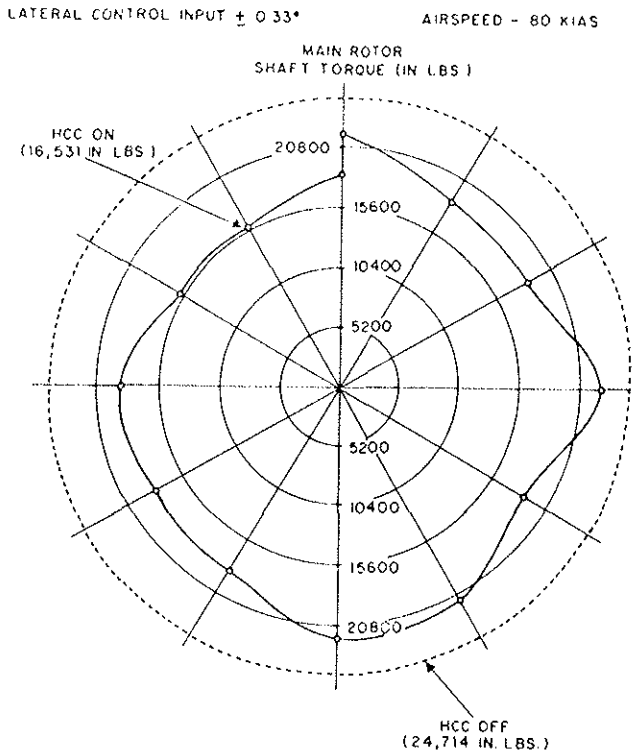

Fig. 5(a) Effect of HHC on main rotor shaft torque at 80 KIAS for lateral input of ± 0.33 degrees.

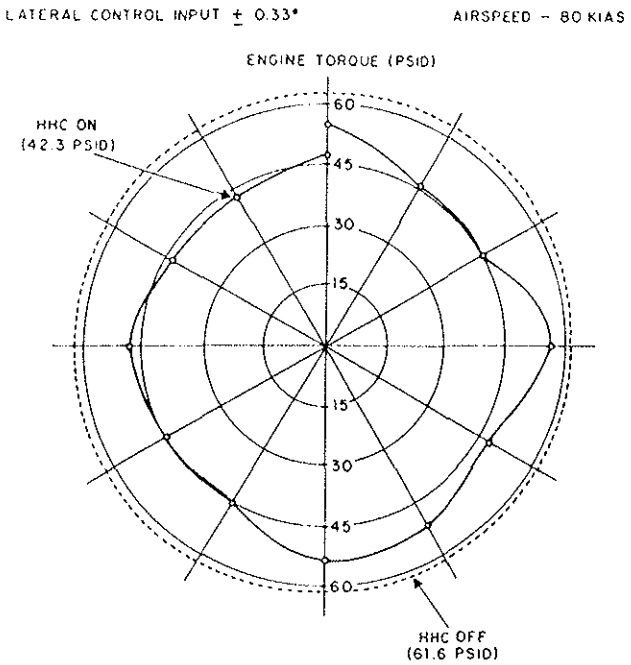

Fig. 5(b) Effect of HHC on engine torque pressure at 80 KIAS for lateral input of ± 0.33 degrees.

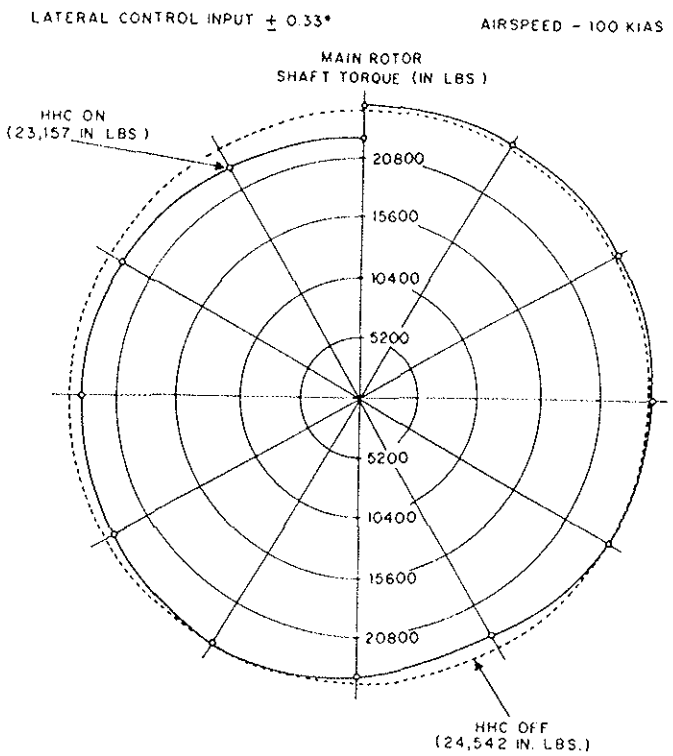

Fig. 6(a) Effect of HHC on main rotor shaft torque at 100 KIAS for lateral input of ± 0.33 degrees.

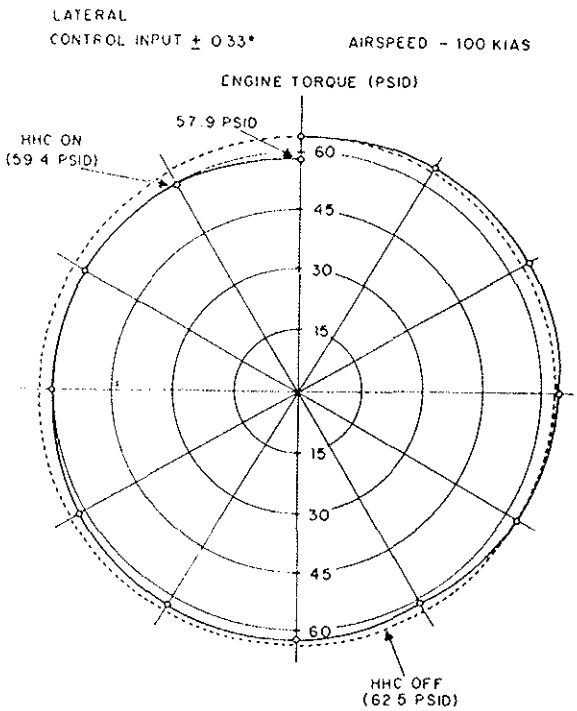

Fig. 6(b) Effect of HHC on engine torque pressure at 100 KIAS for lateral input of ± 0.33 degrees.

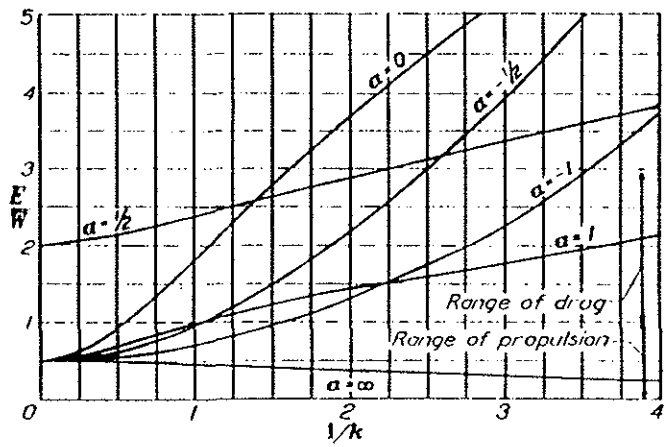

Fig. 7 Garrick's ratio of energy dissipated in wake to the energy required to sustain oscillations for pure pitch about $x=a$.

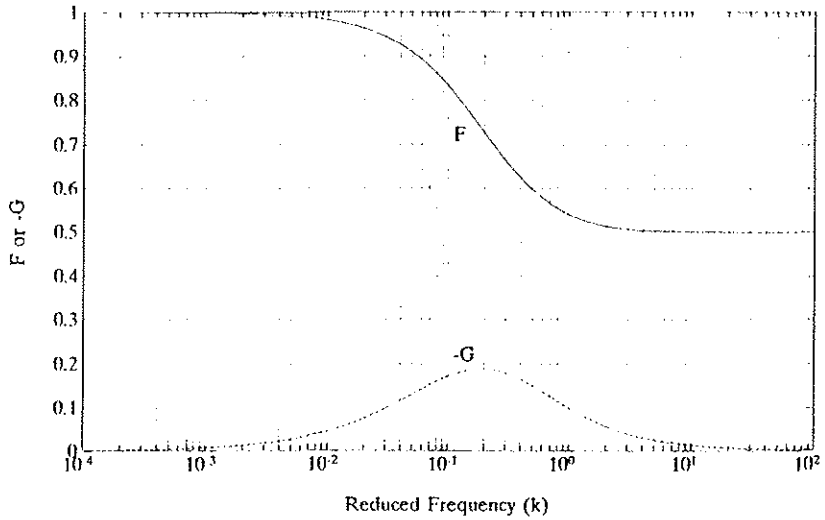

Fig. 8 Theodorsen's lift deficiency function, C(k).

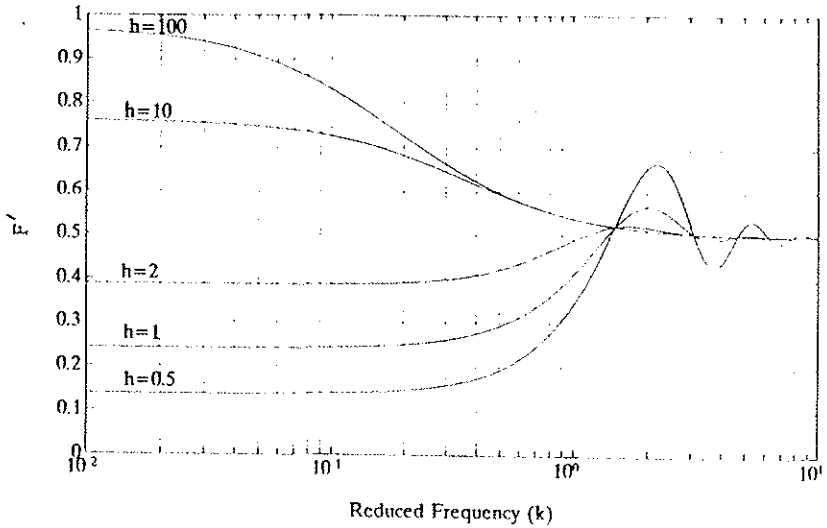

Fig. 9 Loewy's lift deficiency function (real part) as a function of wake spacing for m=0.

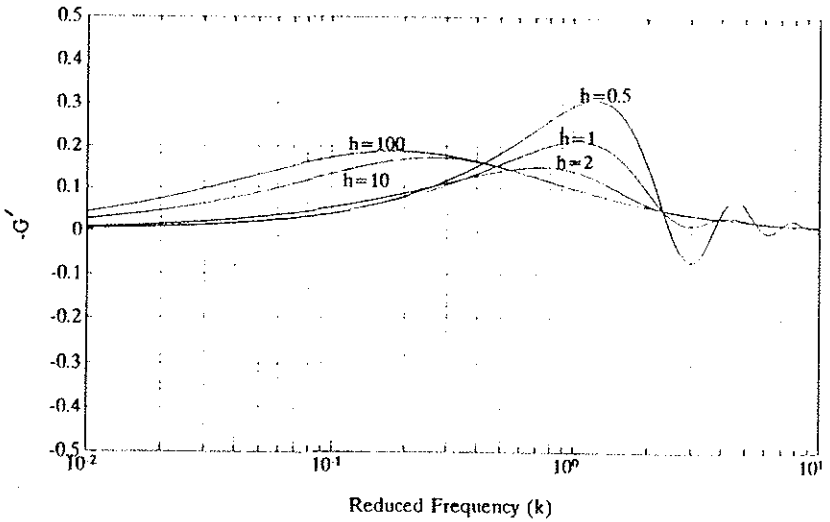

Fig. 10 Loewy's lift deficiency function (imaginary part) as a function of wake spacing for m=0.

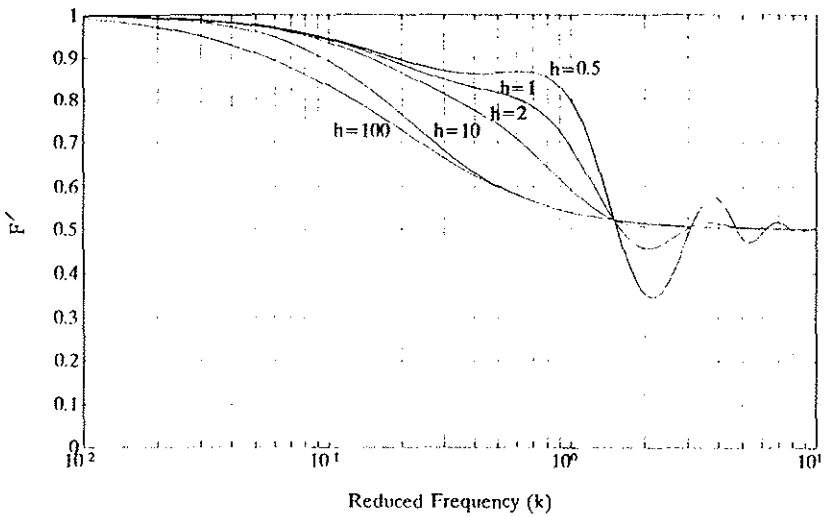

Fig. 11 Loewy's lift deficiency function (real part) as a function of wake spacing for m=0.5.

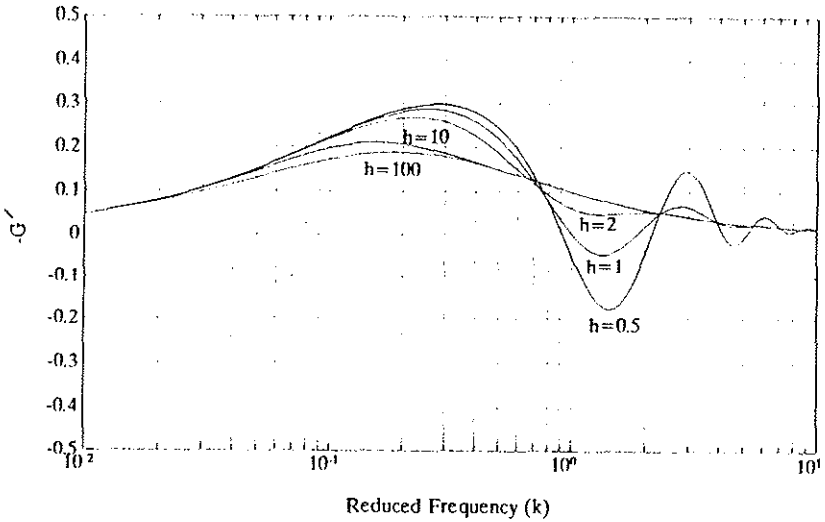

Fig. 12 Loewy's lift deficiency function (imaginary part) as a function of wake spacing for m=0.5.

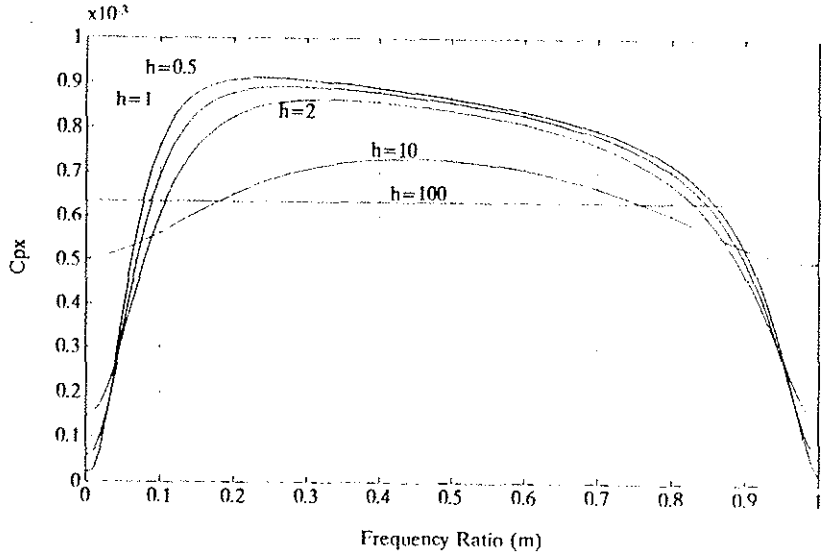

Fig. 13 Propulsive force coefficient in pure plunge as a function of wake spacing using Loewy's lift deficiency function.

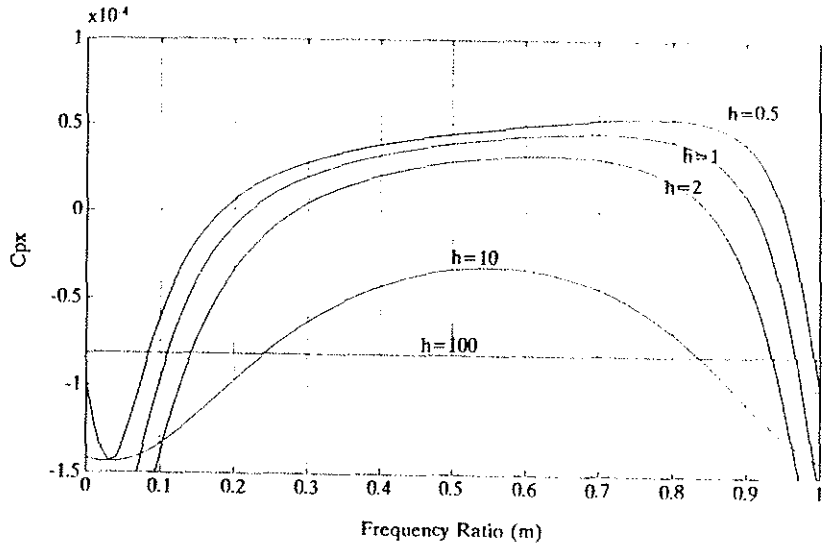

Fig. 14 Propulsive force coefficient in pure pitch as a function of wake spacing using Loewy's lift deficiency function.

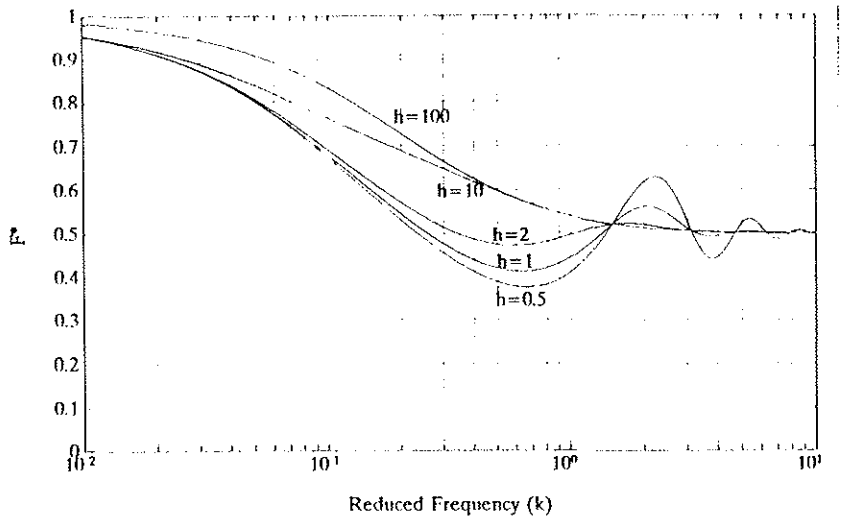

Fig. 15 Single wake lift deficiency function (real part) as a function of wake spacing for m=0.

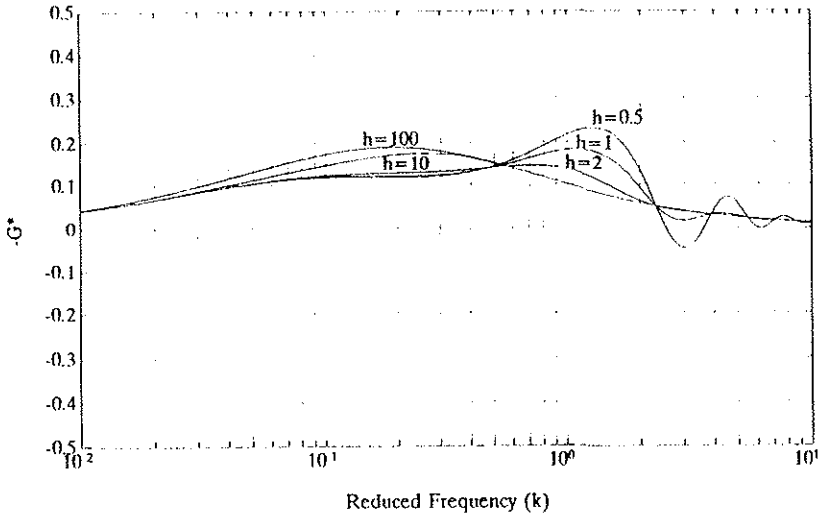

Fig. 16 Single wake lift deficiency function (imaginary part) as a function of wake spacing for m=0.

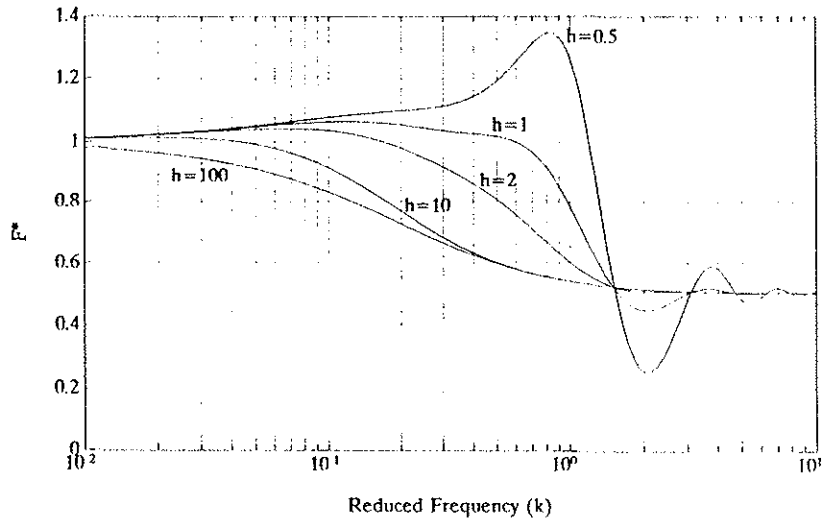

Fig. 17 Single wake lift deficiency function (real part) as a function of wake spacing for m=0.5.

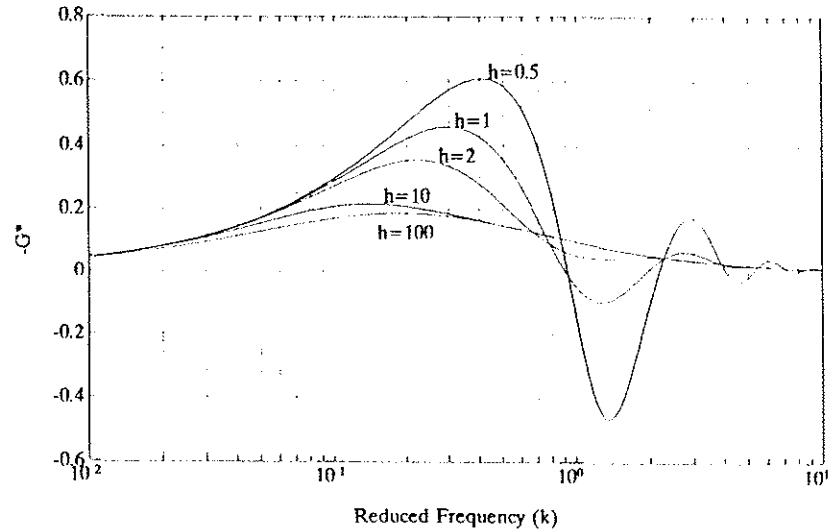

Fig. 18 Single wake lift deficiency function (imaginary part) as a function of wake spacing for m=0.5.

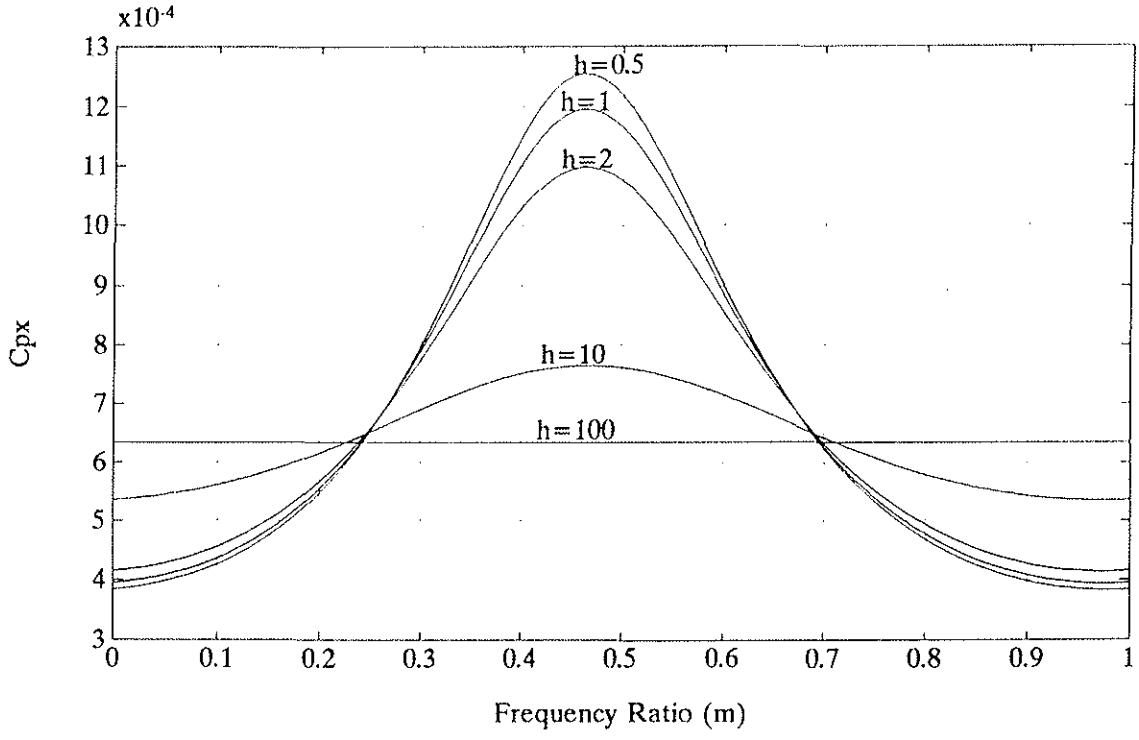

Fig. 19 Propulsive force coefficient in pure plunge as a function of wake spacing using single wake lift deficiency function (k=0.1234, $\bar{h}_o$=0.14).

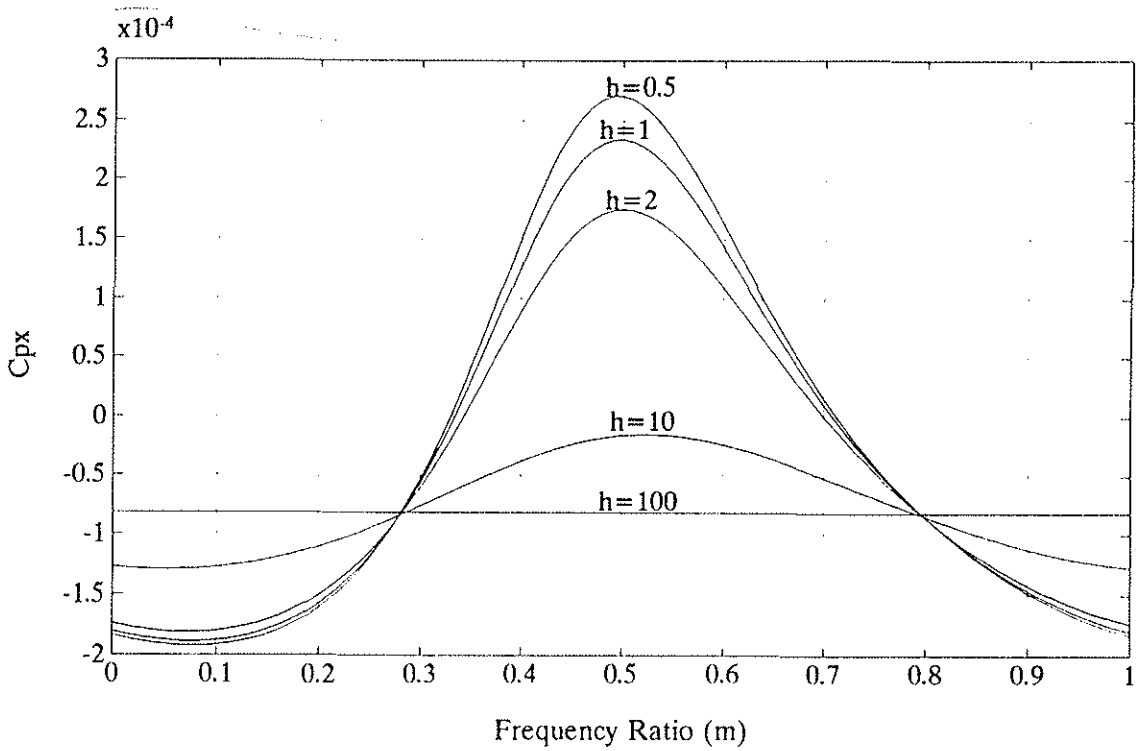

Fig. 20 Propulsive force coefficient in pure pitch as a function of wake spacing using single wake lift deficiency function (k=0.1234, α_o=1°).

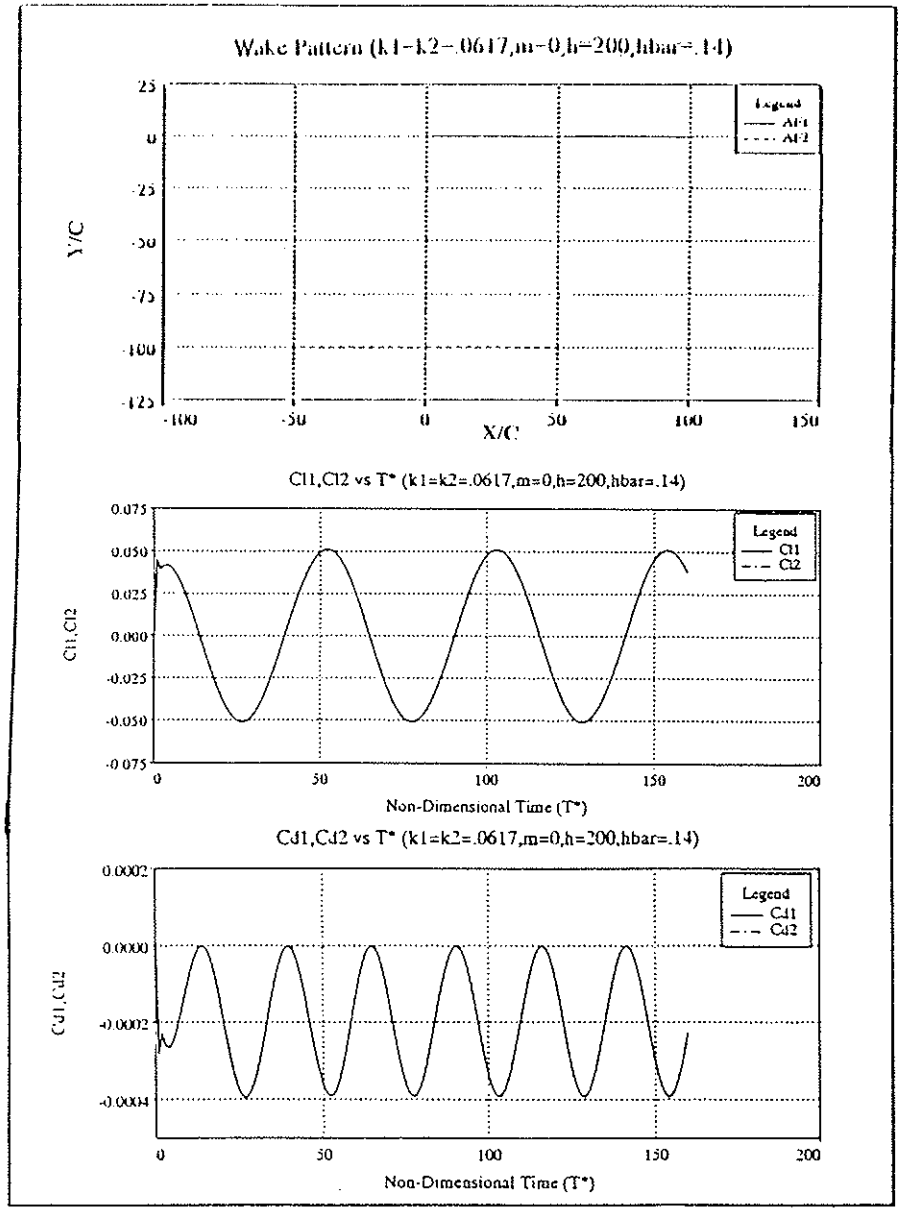

Fig. 21 NPS Panel Code time history of Cl and Cd for h = 200 (wake at infinity).

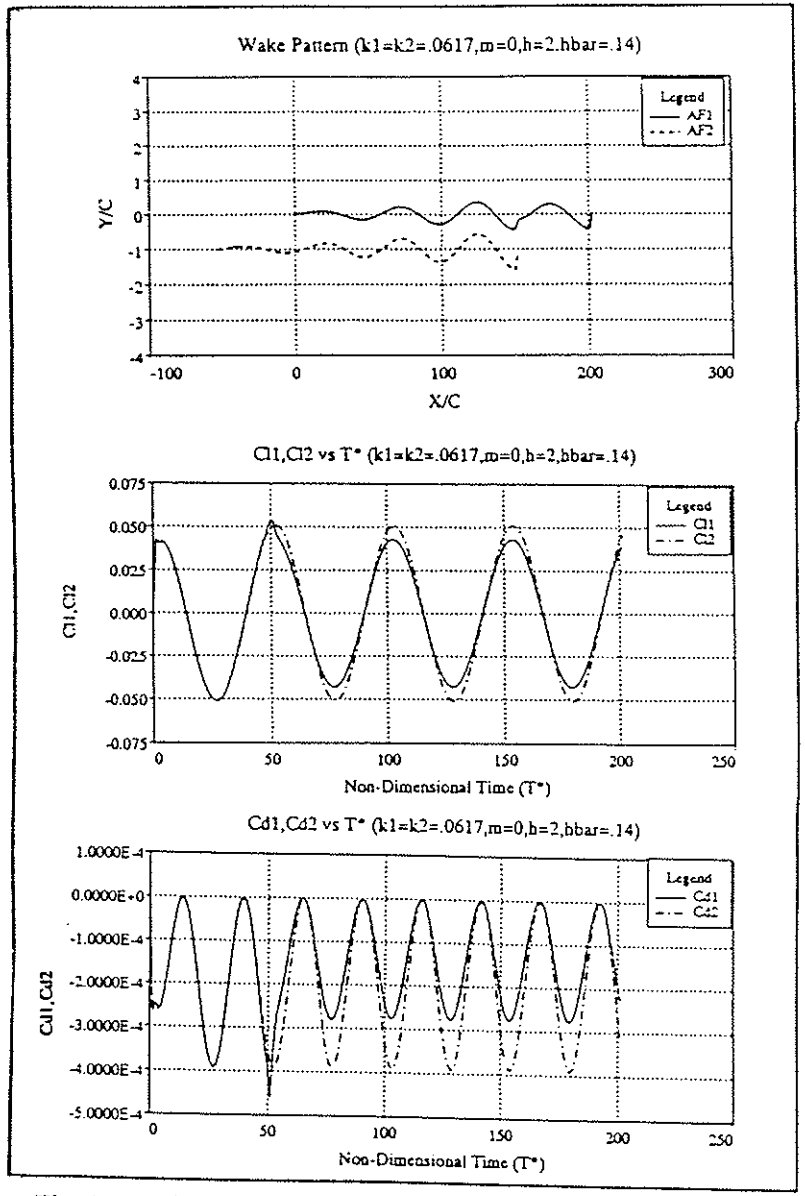

Fig. 22 NPS Panel Code time history of Cl and Cd for h = 2; m = 0.0 (0° phase angle).

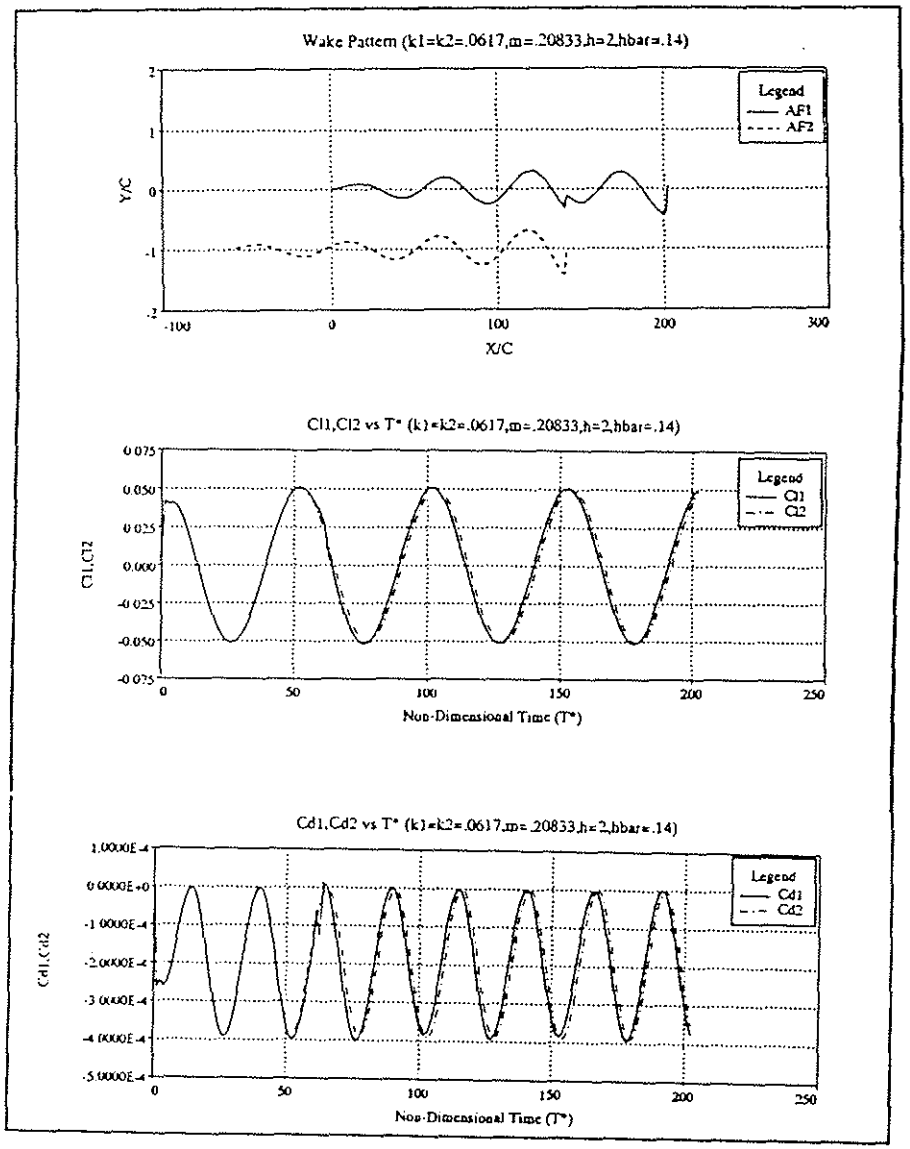

Fig. 23 NPS Panel Code time history of Cl and Cd for h=2; m=.20833 (75 ° phase angle)

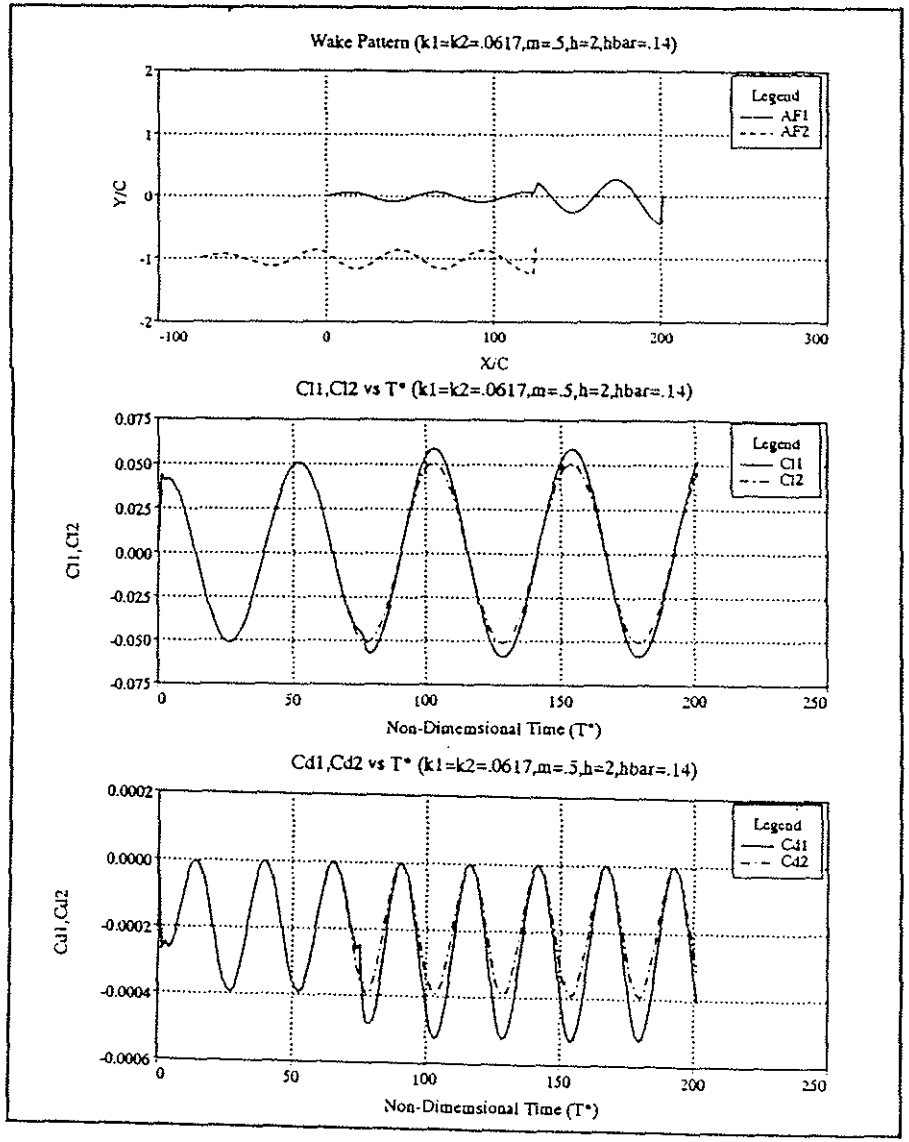

Fig. 24 NPS Panel Code time history of Cl and Cd for h=2; m=. 5 (90 ° phase angle)

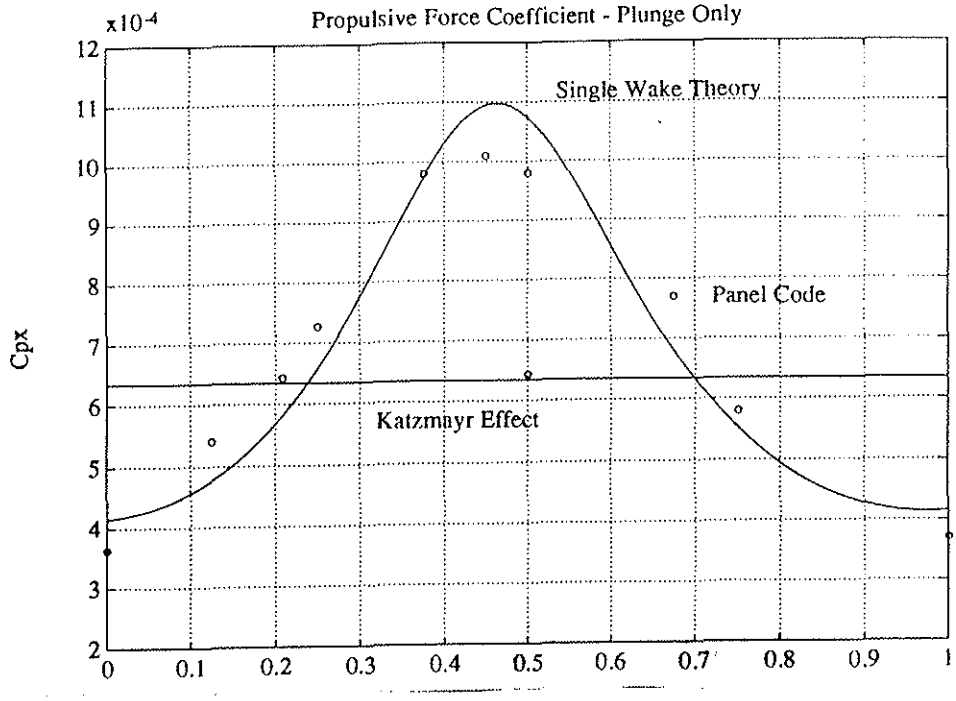

Fig. 25 Comparison of propulsive force coefficient in pure plunge (h=2.0,k=0.1234, $\bar{h}_o$=0.14)

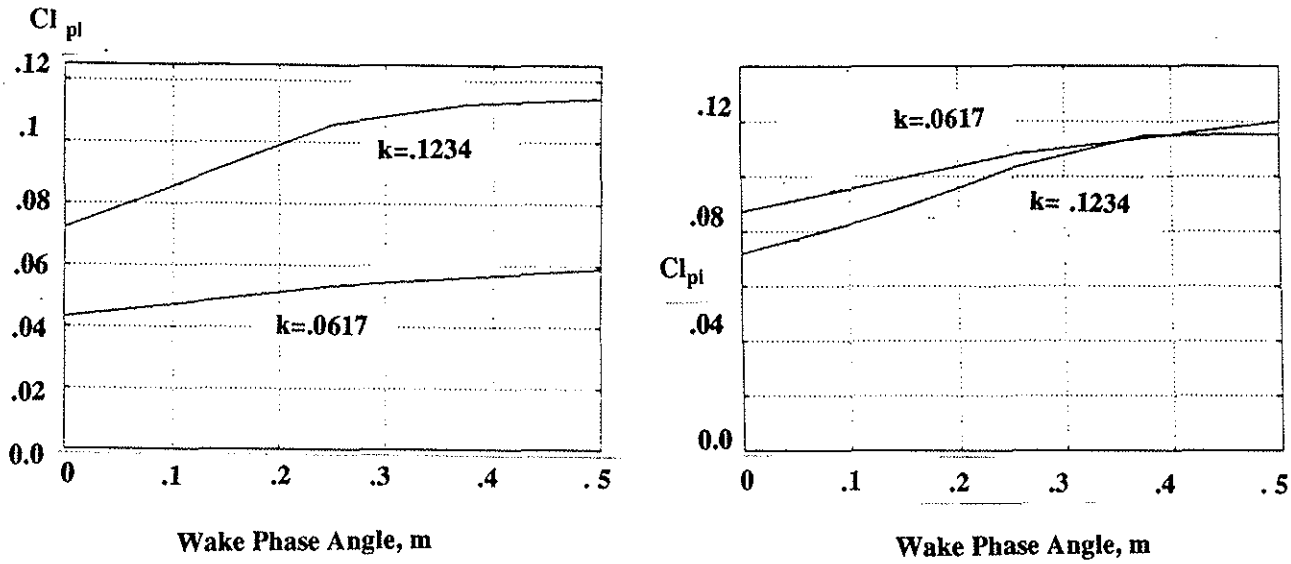

Figs. 26 and 27 Effect of wake phase angle, m, on lift coefficients due to plunge and pitch, respectively.

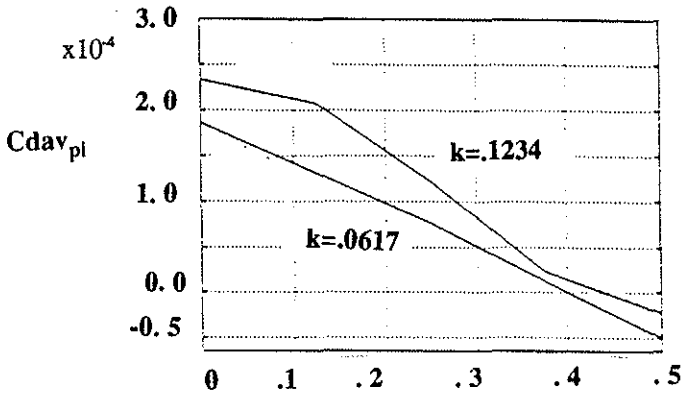

Fig. 28 Effect of phase angle, m, on average drag force due to 1 degree pitch, at h = 2.

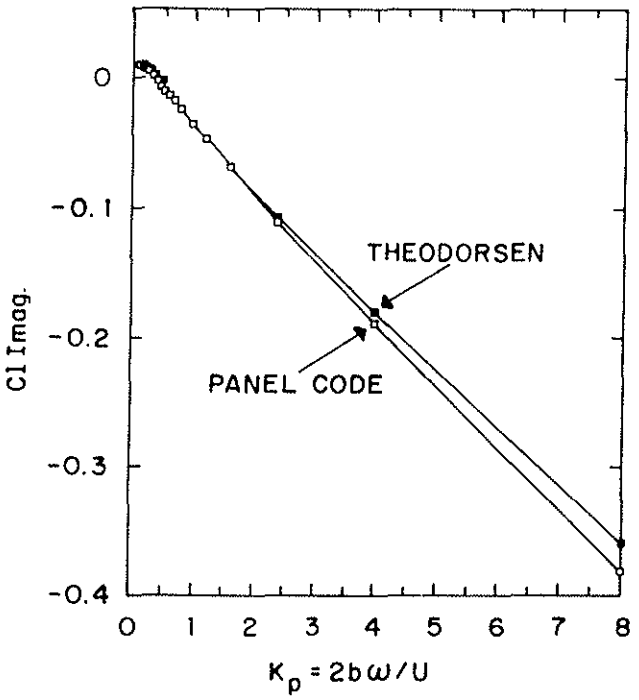

Fig. 29 Comparison of real part of lift coefficient of Theodorsen theory with NPS Unsteady Panel Code; NACA 0007 airfoil; pitch ± 1 degree; N = 75 panels.

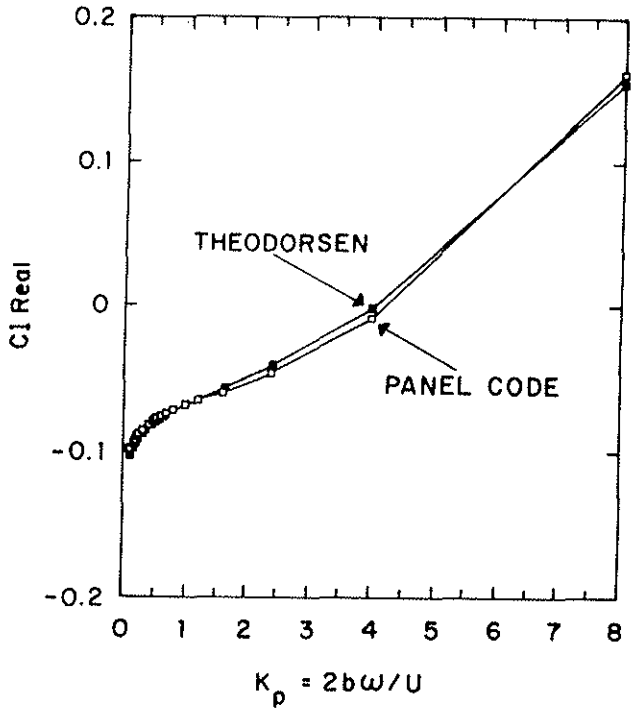

Fig. 30 Comparison of imag. part of lift coefficient of Theodorsen theory with NPS Unsteady Panel Code; NACA 0007 airfoil; pitch ± 1 degree; N = 75 panels.

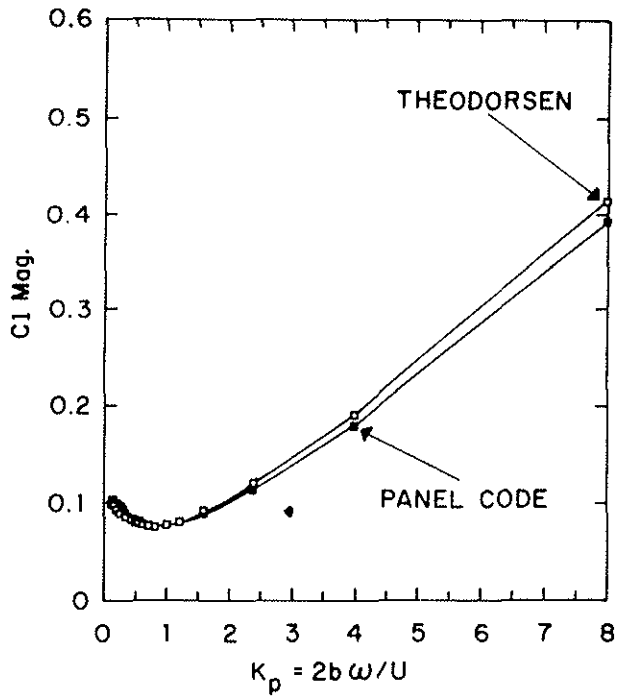

Fig. 31 Comparison of magnitude of lift coefficient of Theodorsen theory with NPS Unsteady Panel Code; NACA 0007 airfoil; pitch ± 1 degree; N = 75 panels.

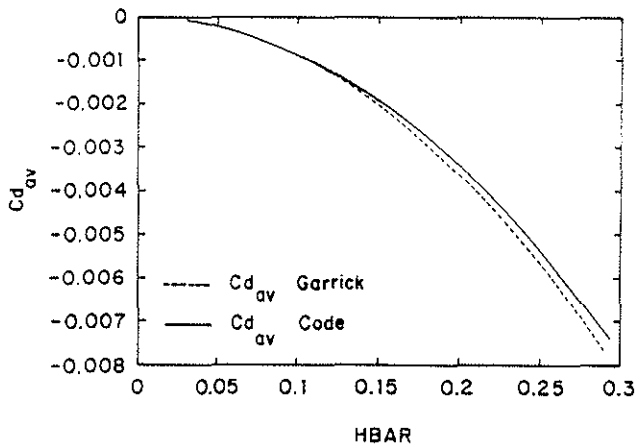

Fig. 32 Comparison of average drag coefficient from Garrick theory with NPS Unsteady Panel Code; versus non-dimensional plunge amplitude;k = 0.05.